PRICES SUBJECT TO CHANGE

COLLEGE OF ENGINEERING

Prairie View A&M University of Texas

Prairie View, Texas   77445

A Final Report

on

RADAR CROSS SECTIONS OF STANDARD
AND COMPLEX SHAPED TARGETS

Research Project: NGL44-033-017

Principal Investigator: M.S. Sohel, PhD.

Submitted to

National Aeronautics and Space Administration

- /-

ACKNOWLEDGEMENTS

ABSTRACT

This study presents in a systematic form the theoretical, analytical, and experimental results of radar-cross-sections of targets of different shapes. This report is designed to give the engineer a feel for the gross features of the target and the resulting radar-cross-section to be expected. This will help him then to begin a detailed analysis inorder to obtain a better prediction of the true RCS of the target. Various techniques useful to predict RCS are given. RCS of finite standard targets is presented. Then a presentation of techniques used to predict the RCS of complex targets is made. Finally, RCS of complex shapes is given. This report will be very helpful to accomplish National Aeronautics and Space Administration goal of predicting the RCS of candidate targets

CONTENTS

3-a

Introduction

Radars were developed by independent efforts of several countries during the early twentieth century. Basically speaking, it is an electronic eye useful:

(1) To detect and locate targets which are obscured to the naked eye because of distance or environmental conditions.

(2) To determine the physical shape of a target, from the knowledge of the incident energy and reflected energy.

(3) To determine the speed of the moving target.

(4) To determine the type of material the target is made of.

(5) To guide airplanes when the pilot is not able to see due to bad weather conditions.

RADAR-CROSS-SECTION

In order for a radar to determine the physical shape of an object, the utilization of the radar-cross-section is employed. Radar-Cross-Section or RCS is defined as 4 times the ratio of the back scattered power per unit solid angle to the incident power per unit area. It maybe noted here that radar-cross-section has units of area and is generally denoted by (σ).

$$\frac{\text{back scattered power/unit solid angle}}{\text{incident power/unit area}}$$

In other words, the reflectivity of the target at which a radar signal is incident is expressed by the radar-cross-section, which includes eddects of area, configuration, size and material of the target.

METHODS OF DETERMINING THE RADAR-CROSS-SECTION

Research on RCS dates as far as 1949. Some of the methods found in the earlier research were used in World War II to determine targets of interest to the United States Military. Some of the earlier methods are:

(1) Using pulse signals and measuring the electric field strength.

(2) Using continious wave (cw) signals and measuring the standing wave distribution or measuring the doppler shift (shifts caused by the effect of target or medium motion whith relative to each other.)

(3) Method

(3) Methods using frequency modulated continious wave signals in frequency modulated radars.

Today, there are techniques such as:

(1) Physical Optics
(2) Geometrical Theory of Diffraction
(3) Creeping Wave Analysis
(4) Impulse Response Theory

Physical optics is used to calculate the radar-cross-section for perfectly conducting bodies. This theory explains the behavior of light and takes into account the phasing between scatters. The physical optics theory arises from the radiation integral which

assumes that the surface current is the same at any point as it would be at that point on an infinite plane tangent to the body at that point and assumes further the existence of a sharp shadow boundary, beyond which surface current is identically zero, Unfortunately, the approzimation is poor at just those parts of the surface of the body that are most important in determining the value of the integral. Therefore, physical optics frequently give poor results.

This theory has certain limitations such as:

(1) When the theory is applied to bistatic cases (transmitter and reciever in different places) it yields results that do not conform to the principles of reciprocity.

(2) Polarization dependence of backscattering cannot be obtained from using this method.

(3) Physical optics is unable to account for effects for arising from diffraction or creeping-wave progation into the shadow region of a body.

However, physical optics is still used despite it limitations. It is used because in some cases it gives good results such as for perfectly conducting bodies and most of the time can tell in advance for which cases these results can be obtained.

The physical-optics cross section for backscattering of a body' is given by this expression: (Ross, 1966)

$$\sigma = 4\pi \, |g(k)|^2$$

$$g(k) = \frac{-jk}{2\pi} \int dz \, \frac{da}{dz} \, e^{jkz}$$

Where:

    k = wave number = $2\pi/\lambda$
    λ = radar wavelength
    z = coordinate along the radar line of sight
    A = area of intercept of body with plane perpendicular to radar line of sight

However, the expression just sited to give poor results for
bistatic scattering. Various methods have been suggested for the
modification of physical optics so that it will yield better results.
Such suggestions as: modifying the assumed surface currents, or
the method used by S. Adachi, which was to continue the integration
over the total surface instead of over just the illiminated portion.
However, Adachi (1965) method proved rather odd results.

Physical Optics can lead to serious error, mainly because it
assumes that the current distribution on a surface is the same at
each point.

The most practical of the asymptotic techniques that have been
developed so far is the geometrical theory of diffraction, developed
poincipally by J. B. Keller (1960). This theory takes into account
diffracted, as well as reflected rays. Geometrical diffraction
theory assumes localization of the scattering at points defined
by stationary phase arguments or by abrupt geometric discontinuities.
Also, the current distribution of a scattering center is obtainable
from that of a known case of similar geometry. Then based on similar
known problems a diffraction coefficient is assigned to each center.
This coefficient is the function of a phaser proportional to the
distance along a ray projected from the scattering center to the
radar.

Even though, this theory is practical for many targets it is
not yet related to Maxwell's equations. Also, the prediction of
cross section near grazing incidence is a problem for the geometri-
cal theory of diffraction. The results from this theory approaches

infinity near edge on aspect angles due to singularities contained in terms describing multireflections. The effect of multireflections issnot discussed in this study, because radar-cross-section of the target to be considered in this study can be predicted by the scattering centers in term of single diffraction.

Moreover, the geometrical theory of diffraction has been applied to predict RCS of such bodies as spheres, rectangular flat plates and cones. The theory provides good results except for the nose on aspect angles.

The creeping wave theory is concerned with the waves that passes around the rear of a smooth body. This theory is of importance mainly for small bodies, generally in the resonance region, or for bodies specifically constructed to have low radar-cross-section. The theory is valid for the resonance region mainly because the creeping wave tends to become very small after progating a few wavelengths. The creeping-wave contributions to cross-sections are generally small, ther are usually important for bodies that do not have large scatters on them.

There are two methods for computing the creeping-wace contributions to radar scattering. First, one can perform an asymptotic expansion of the exact solution of the scattering problem and recognize the creeping-wave contributions in the answer through the phase expressions that appear in the answer. However, here one needs the exact solution to the scattering. Second, one can use the geometrical theory of diffraction approach. This method uses

the diffraction and decay coefficients so obtained from the geometrical theory of diffraction to calculate the contribution from the creeping-wave.

The impulse-response technique was developed by Kennaugh (1965). This method considers the scattering of a short pulse, an impulse, a step function, or a ramp function rather than the continious wave or short oscillatory pulse normally considered. The method is similar to the impulse-response method used in the investigations of the transient behavior of physical systems such as servomechnisms.

It is noted here that an impulse function can only be approximated and the ideal impulse is not normally generated. Therefore, the hypothetical impulse is not oscillatory, so the entire surface of the body contributes to the scattering. Frim linear systems analsis, it is khown that convolution techniques can be used to derive continious waves or short oscillatory pulses from the impulse response.

The impulse-response technique is capable of bridging the gap between Rayleigh scattering and high frequency results into the lower-frequency region, physical optics and geometrical diffraction theory results can thus be made to hold quite well in the resonance region. The impulse-response theory also takes into account com- binations of simple shapes and the distortion of a simple shape into a more complex one. This technique permits the use of different computational techniques for diffrent parts of the body, since the impulse response for each region of the body can be added together.

The advantages of the impulse-response technique are:

1) Its ability to treat scattering in the resonance region
2) The simple pictures it gives of scattering
3) The ease in which computational methods can be used
4) Its experimental results can be used to improve the
    results of analytical techniques.

The geometrical theory of diffraction produces good results for many bodies. It has been applied to such bodies as; flat plates, right circular cones, cylinder, frustrums and other bodies. The theory also provides good results for complex and composite bodies.

Moreover, the radar-cross-section of composite bodies such as service satellites, missles and other such bodies are of great concern. This paper will present the radar-cross-section of a missle, by the use of the geometrical theory of diffraction.

APPLICATION OF GEOMETRICAL DIFRACTION THEORY TO SCATTERING FROM CONES AND DISKS

The study compares the previous analytical results, obtained by geometrical theory of diffraction for perfectly conducting cones and disks, with experimental results for both horizontal and vertical polarization cases. Presentation is made for cones ranging from 0.98 to 2.87 wavelengths in diameter at the base and having half angles of 4°, 15°, and 90°, the latter corresponds to a disk.

TARGET GEOMETRY AND COORDINATE SYSTEM

The target geometry and coordinate system used is presented in Figure 1.

ANALYTICAL AND/OR EXPERIMENTAL PLOTS

The analytical and experimental results are plotted in Figures 2. through 13.

INTERPRETATION OF RESULTS

The results seem to agree well. Futhermore, for cones having normalized base circumference (ka) of 8 or 9, the predicted and measured RCS agree well except when the cone is observed within about 30° of nose-on for vertical polarization, in which case large errors occur for some as yet unknown reason. For smaller cones having diameters about equal to the wavelength (ka around 3), the computed RCS is generally pre-

dicted within 5dB, but the form of RCS is not predicted very accurately. Baskscattering from a disk of the same diameter for viewing angles within 60° of the normal to the base.
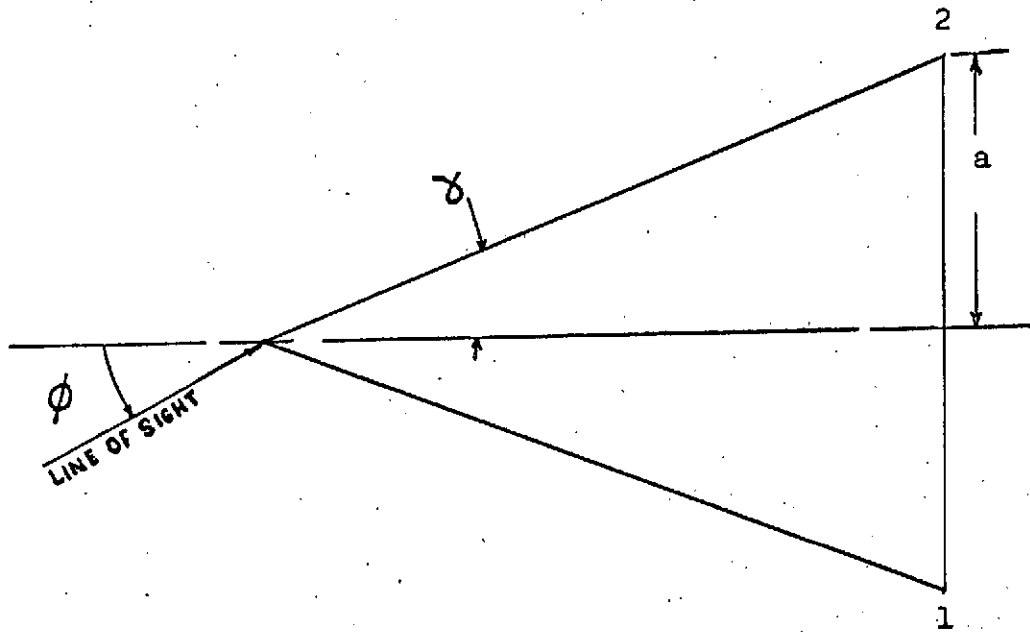
Fig.1. Longitudinal section of a right circular cone.
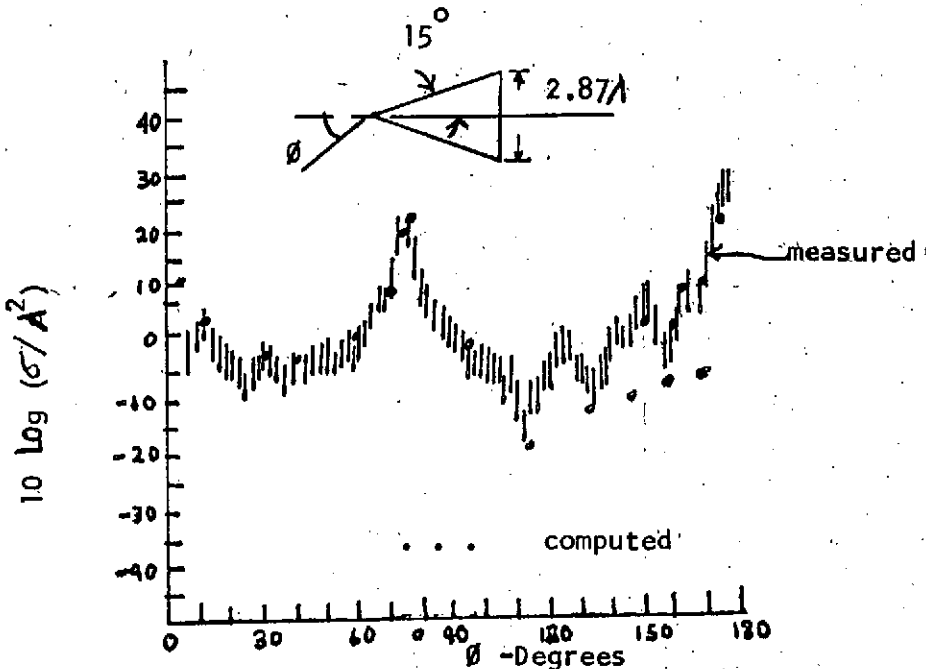
Fig. 2. Vertically polarized RCS for cone;
$\gamma = 15°$ ka=9.02.

Fig. 3. Horizontally polarized RCS for cone
$\gamma = 15°$, ka=9.02.
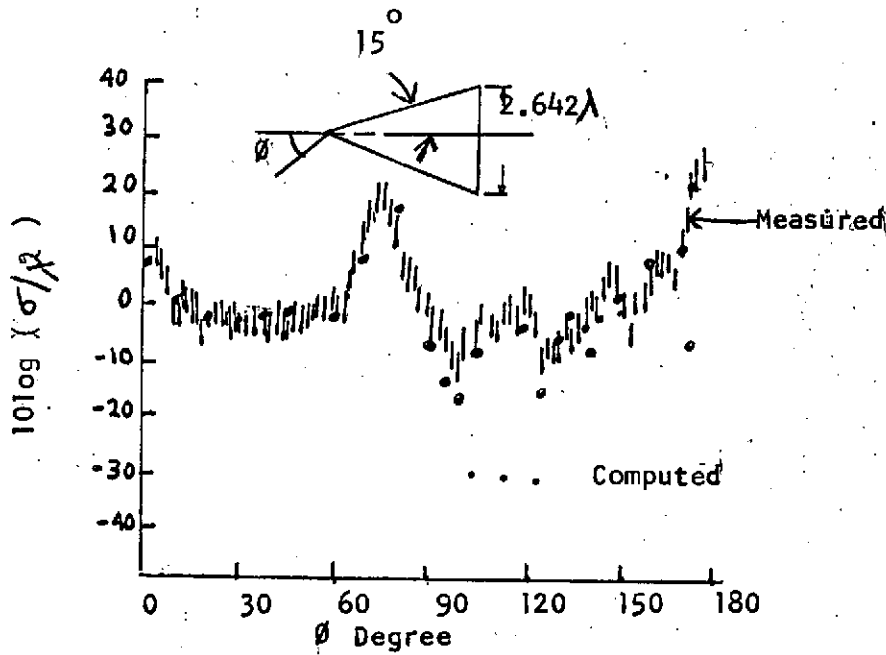
Fig. 4.. Veritically polarized RCS for cone; γ=15^0, ka=8.28.

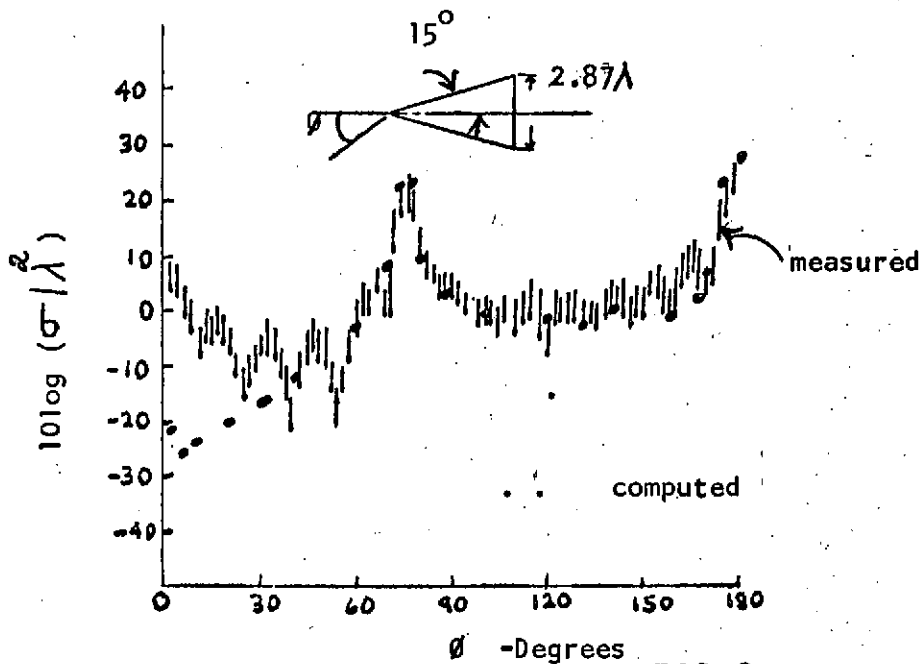Fig. 5. Horizonitally polarized RCS for cone; γ=15^0, ka=8.28.
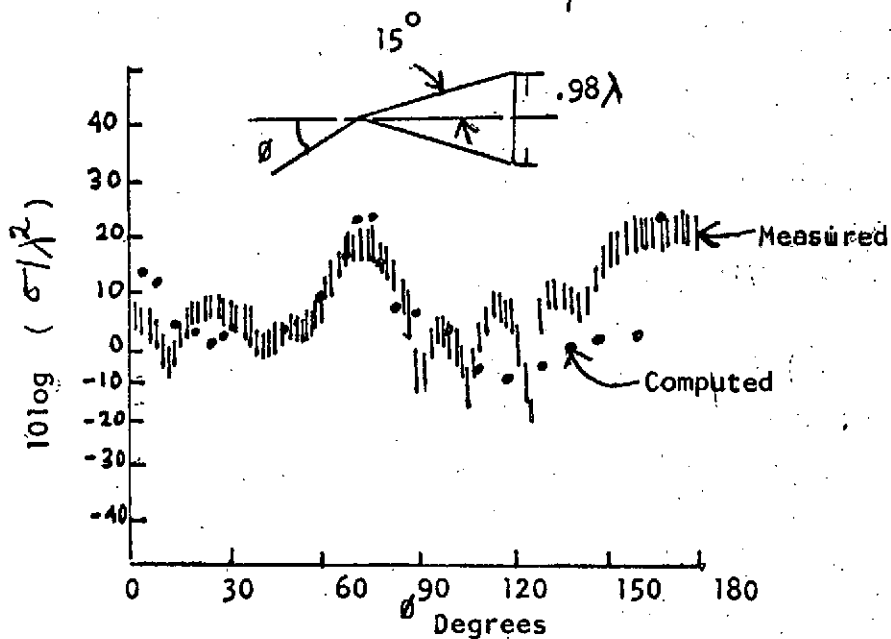
Fig. 6. Vertically polarized RCS for cone; $\gamma=15^{\circ}$, ka=3.08

Fig. 7. Horizontially polarized RCS for cone; $\gamma=15^{\circ}$, ka=3.08.
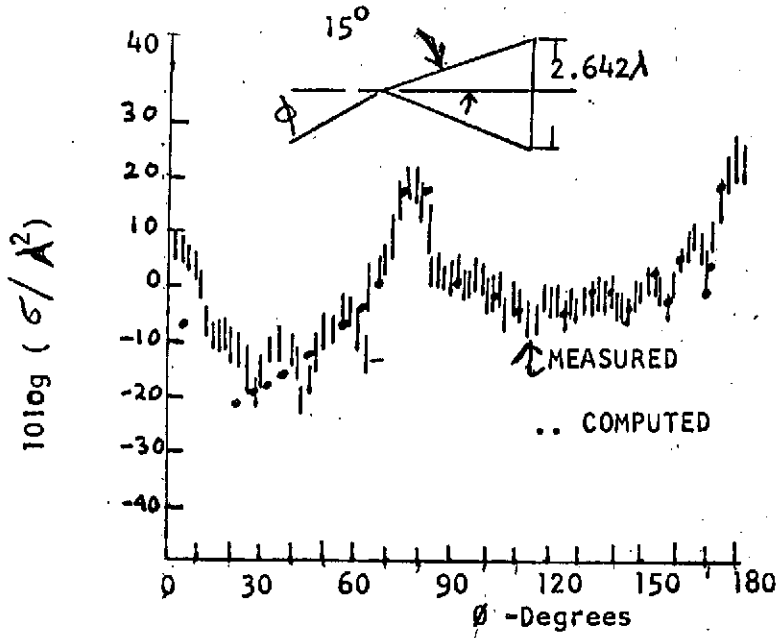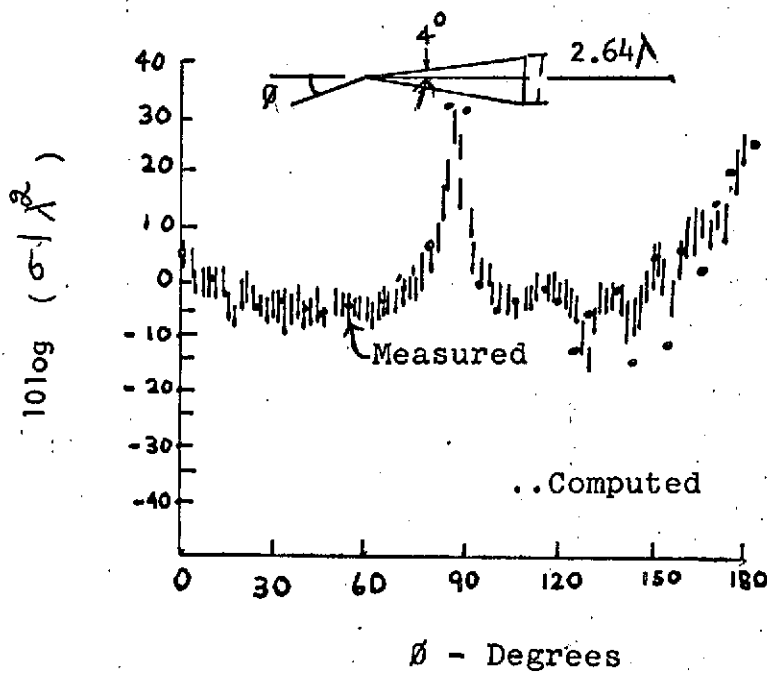
Fig. 8. Veritically Polarized RCS for cone; $\gamma = 4^{\circ}$, ka=8.28.
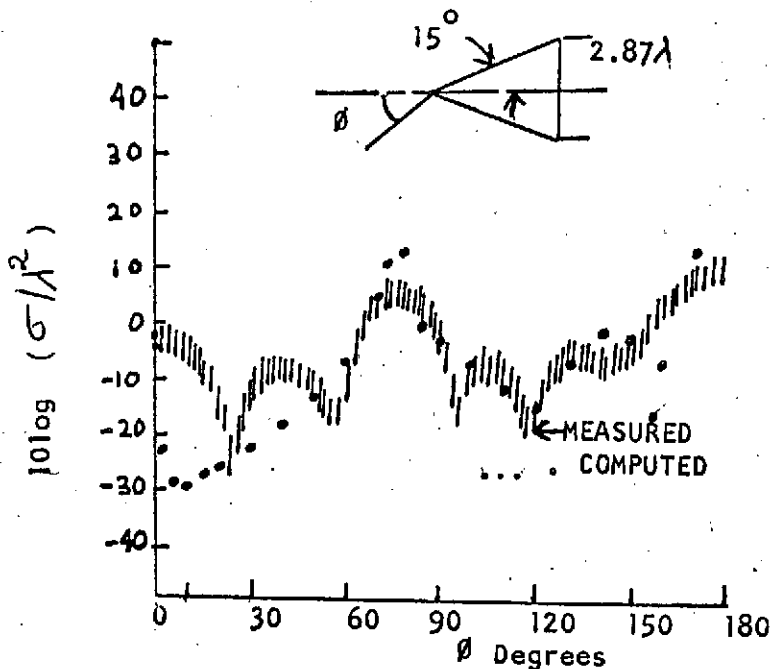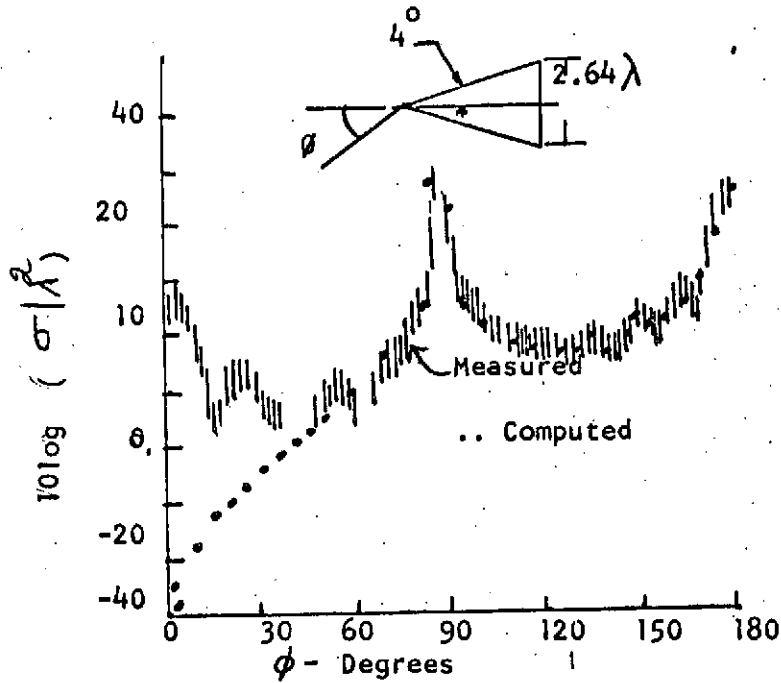
Fig. 9. Horizontally polarized RCS for cone; $\gamma = 4^{\circ}$, ka=8.28.
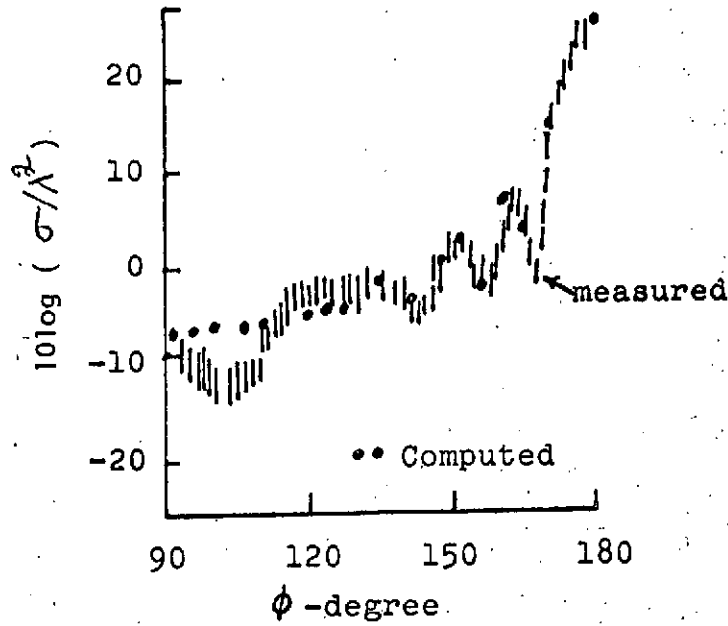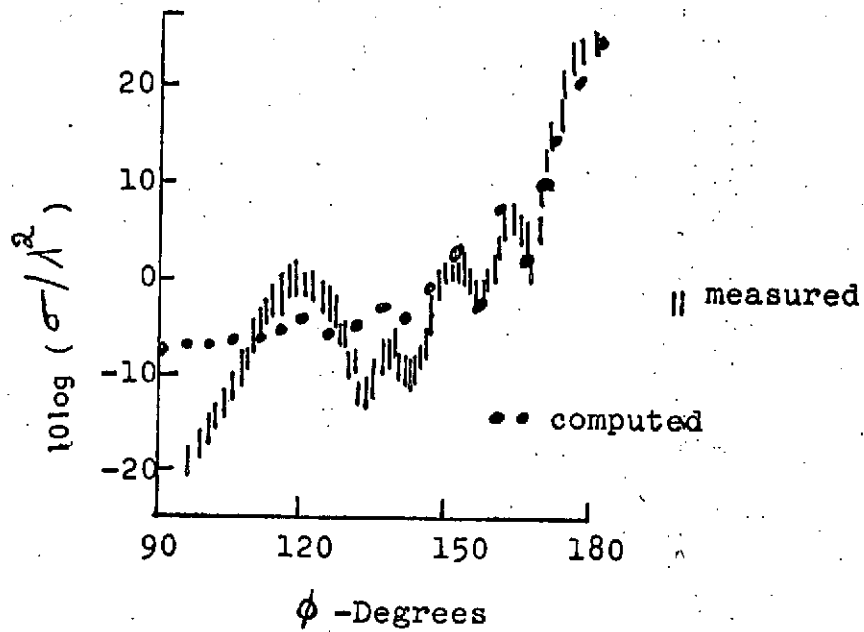
Fig. 10. Vertically polarized RCS for disk; ka=8.28

Fig. 11. Horizontally polarized RCS for disk; ka=8.28.
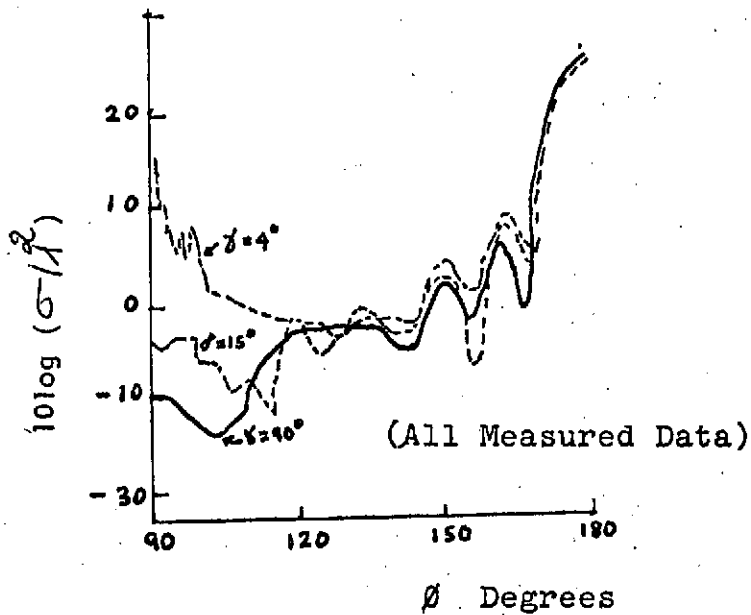
Fig. 12. Measured vertically polarized RCS of cones; ka=8.28
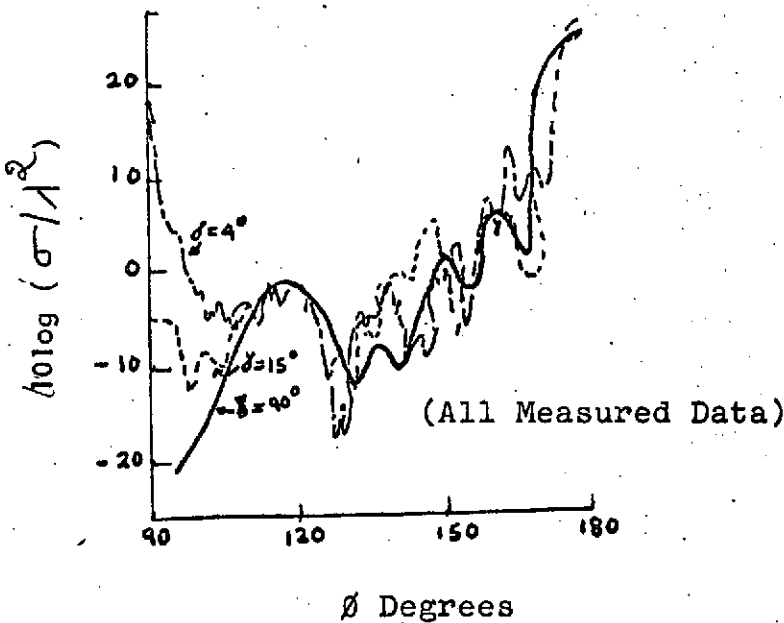
Fig. 13. Measured horizontally polarized RCS of cones; ka=8.28

RADAR-CROSS-SECTION OF RECTANGULAR FLAT PLATES AS A FUNCTION OF ASPECT ANGLE

This study investigates the scattering from flat perfectly conducting plates. Radar-Cross-Section results are presented, based upon both theoretical as well as experimental studies. RCS expressions based upon physical optics theory for near specular returns are presented. Geometrical theory of diffraction gives good results for non-specular cases except for edge on case. Based upon experimental measurements, an analytical expression is derived from this data for edge-on case.

TARGET AND COORDINATE SYSTEM

The target (perfectly conducting rectangular flat plate) and coordinate system used is shown in Fig. 1.

ANALYTICAL EXPRESSIONS

Based upon optics theory, an expression of the RCS, for both horizontal and vertical polarization may be written as:

$$\sigma_{p.o.} = \frac{64\pi a^2 b^2}{\lambda^2} \cos^2\phi \left[\frac{\sin(2ka\sin\phi)}{(2ka\sin\phi)}\right]^2$$

Futhermore, based upon geometric diffraction theory, the RCS expressions may be written:

For the vertical polarization case:

$$\sigma_{V_{g.d.}} = \frac{4b^2}{\pi} \left| \left[\cos 2ka\sin\phi - \frac{j\sin 2ka\sin\phi}{\sin\phi} \right] - \frac{e^{jka-j\pi/4}}{\sqrt{2\pi}(2ka)^{3/2}} \left[\frac{1}{\cos\phi} + \frac{e^{j2ka-j\pi/4}}{4\sqrt{2\pi}(2ka)^{3/2}} \left(\frac{(1+\sin\phi)e^{-j2ka\sin\phi}}{(1-\sin^2\phi)} + \frac{(1-\sin\phi)e^{+2jka\sin\phi}}{(1+\sin^2\phi)} \right) \right] \times \left[1 - \frac{e^{j4ka-j\pi/2}}{8\pi(2ka)^3} \right]^{-1} \right|^2$$

and for the horizontal polarization case:

$$\sigma_{H_{g.d.}} = \frac{4b^2}{\pi} \left| \left[\cos 2ka\sin\phi + \frac{j\sin 2ka\sin\phi}{\sin\phi} \right] - \frac{4e^{j2ka+j\pi/4}}{\sqrt{2\pi}(2ka)^{1/2}} \times \left[\frac{1}{\cos\phi} - \frac{e^{j2ka+j\pi/4}}{2\sqrt{2\pi}(2ka)^{1/2}} \left(\frac{e^{-j2ka\sin\phi}}{1-\sin\phi} + \frac{e^{j2ka\sin\phi}}{1+\sin\phi} \right) \right] \times \left[1 - \frac{e^{j4ka-j\pi/2}}{2\pi(2ka)} \right]^{-1} \right|^2$$

EXPERIMENTAL DETAILS

Three targets (aluminum material) are fabricated for monostatic measurements on the Cornell Aeronautical Labs X-band CW radar range at 1.28 inches wavelength. The dimensions of the plate are shown in the respective figures.

ANALYTICAL AND/OR EXPERIMENTAL PLOTS

Figures 2 and 3 show the plots obtained from the measured and analytical data.

Futhermore, experiment was carried out to measure RCS at grazing indidence (ϕ=90°). Results are shown in figure 4.

An analytical fit to the experimental data show the following accurate expression:

$$\sigma\,(\phi=90°) \;=\; {}^{a}\!/_{\lambda}\; b^{2}\left[\left(1+{}^{\pi}\!/_{2}{}^{x}\;{}^{1}\!/\;(2a/\lambda)^{2}\right)\right.$$

$$\left.+\;\left(1-\frac{\pi}{2}\,\frac{1}{(2a/\lambda)^{2}}\right)\cos\left(4ka-\frac{3\pi}{5}\right)\right]$$

for the vertical polarization case and

$$\sigma_{H}\,(\phi=90°)\;=\;0$$

for the horizontal polarization case.

INTERPRETATION OF RESULTS

A comparasion of the results shows that physical optics theory is valid for a near specular aspect angle incident, whereas geometrical theory of diffraction is valid for $30°\leqslant\phi\leq 80°$ but fails for grazing incidence, i. e., for $\phi\gtrless 78°$. An empirical formular obtained from the expremental results shows good fit for grazing incidents on a flat finite rectangular plate. Futher work needs to be done in the area of deriving modified diffraction coefficients at near grazing incidents.
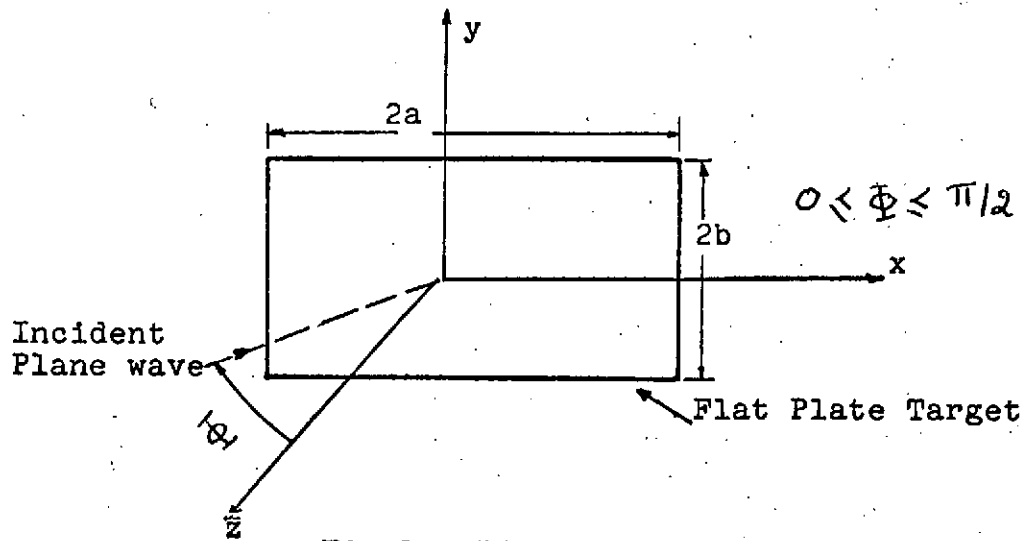
Fig.1. Limitation on aspect angle.
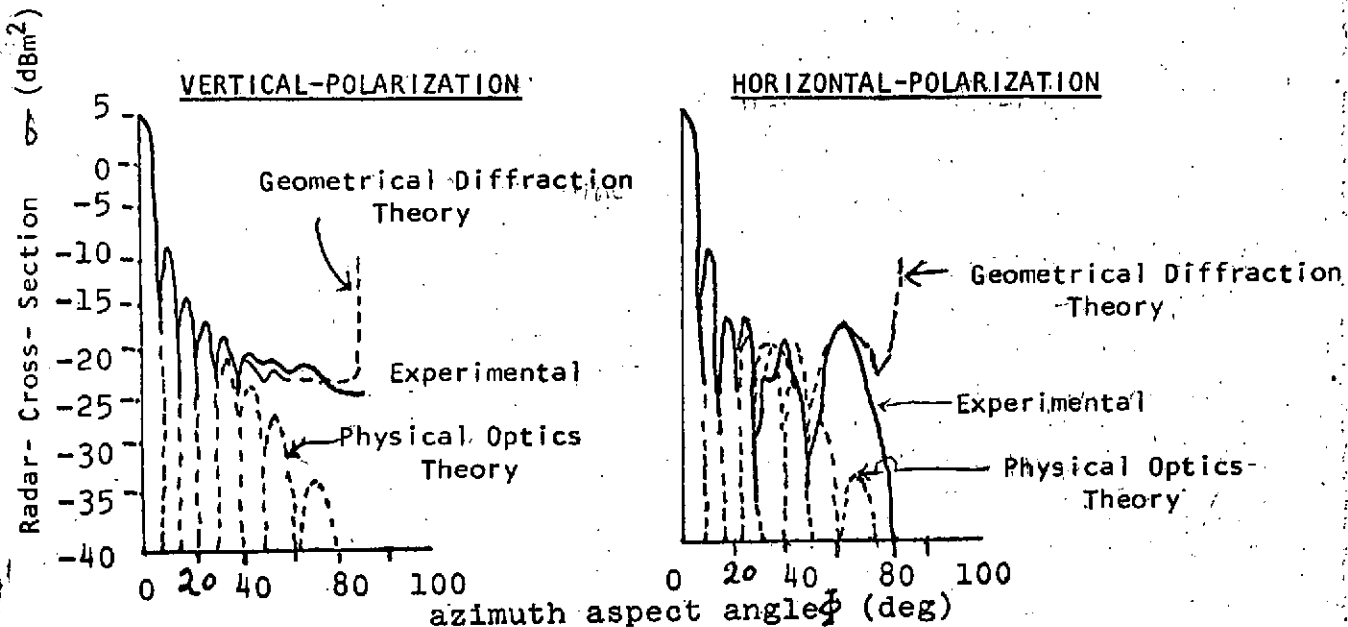
Fig. 4. Cross section of 5X5 inch flat plate (λ=1.28in.).
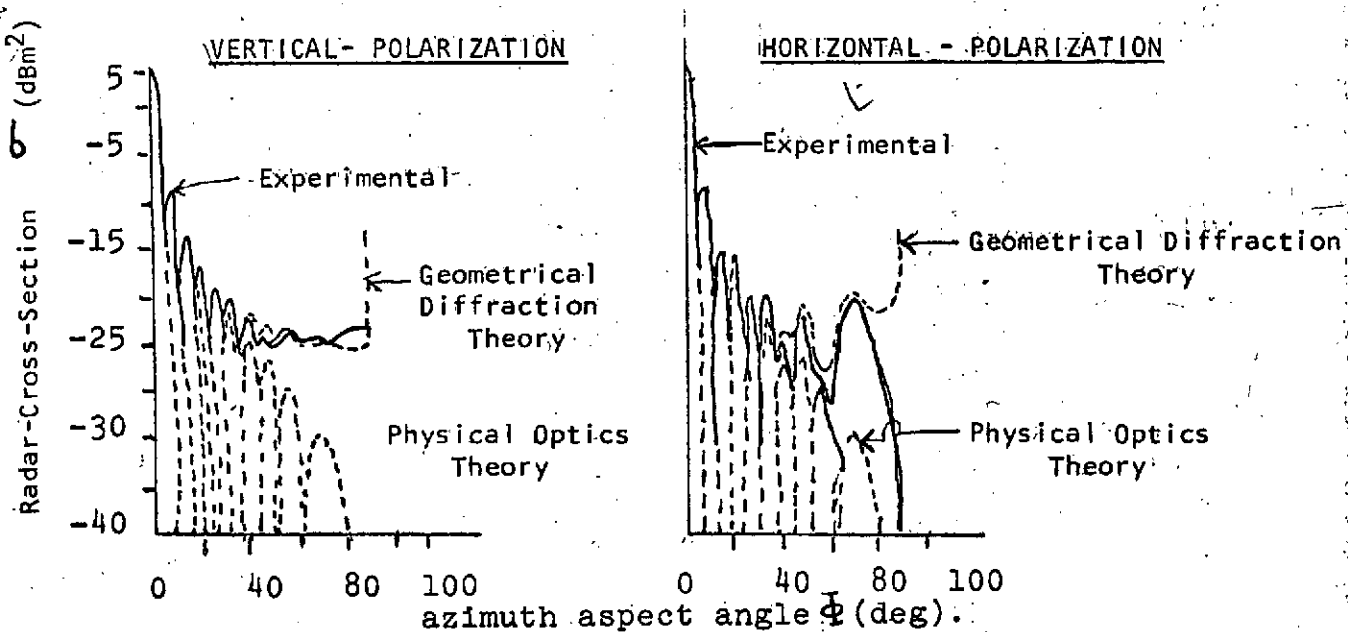
Fig. 5. Cross section of 6.5X¢.5 inch flat plate (λ=1.28in.).
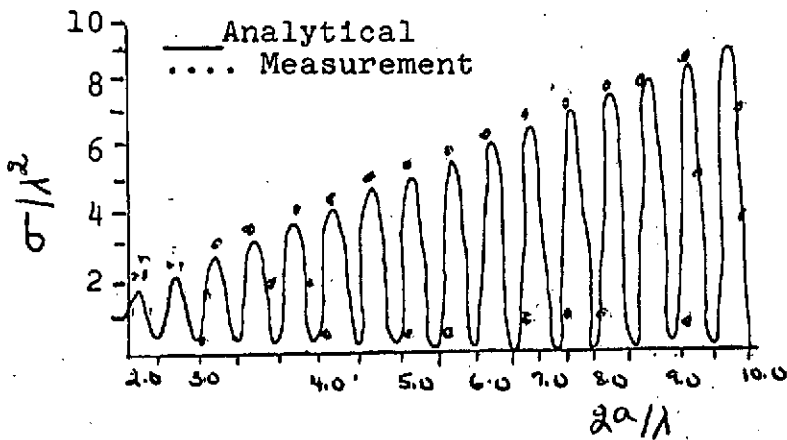
Fig.4. Comparision of analytical fit with measurement data, vertical polarization

BISTATIC SCATTERING MATRIX FOR A FRUSTUM

Keller's geometrical theory of diffraction is applied to derive theoretically the radar-cross-section expressions of a frustum as a function of frequency, aspect angle and bistatic angle. The calculated results from these expressions are in good agreement with the bistatic measurement data.

TARGET AND COORDINATE SYSTEM

The target (perfectly conducting frustrum) and the coordinate system used is shown in Fig. 1.

ANALYTICAL EXPRESSIONS

Symmetry of the problem shows that there are four scattering centers, and the radar-cross-section expressions for them may be written as:

$$\sqrt{\sigma}\; e^{j\rho} = \sum_{i=1}^{4} \sqrt{\sigma_i}\; e^{j f_i} \tag{1}$$

where σ = RCS and f = phase of the scattered field.

Futhermore

$$\sqrt{\sigma_1} = \begin{cases} \dfrac{\sin(\pi/\eta_1)}{\eta_1}\sqrt{\dfrac{a_1\cos\phi}{k\cos(\beta_a/2)}}\left[\left\{\cos(\pi/\eta_1)-\cos\left(\dfrac{\pi+2\phi}{\eta_1}\right)\right\}^{-1} \\ \qquad + \left\{\cos(\pi/\eta_1)-\cos(\beta_a/\eta_1)\right\}^{-1}\right], & \phi \leqslant \pi-\alpha-\dfrac{\beta_a}{2} \\[2mm] 0, & \phi \geqslant \pi-\alpha-\beta_a/2 \end{cases} \tag{2}$$

$$\sqrt{\sigma_2} = \begin{cases} \dfrac{\sin(\pi/n_2)}{n_2} \sqrt{\dfrac{a_2 \csc\phi}{k \cos(\beta_a/2)}} \left[\left\{ \cos(\pi/n_2) - \cos\left(\dfrac{3\pi-2\phi}{n_2}\right) \right\}^{-1} \right. \\ \qquad \left. \mp \left\{ \cos(\pi/n_2) - \cos(\beta_a/2) \right\}^{-1} \right], \quad \phi \geqslant -\alpha + \dfrac{\beta_a}{2} \\[10pt] 0, \qquad \phi < -\alpha + \beta_a/2 \end{cases}$$

$$\tag{3}$$

$$\sqrt{\sigma_3} = \begin{cases} \dfrac{\sin(\pi/n_1)}{n_1} \sqrt{\dfrac{a_1 \csc\phi}{k \cos(\beta_a/2)}} \left[\left\{ \cos(\pi/n_1) - \cos\left(\dfrac{\pi-2\phi}{n_1}\right) \right\}^{-1} \right. \\ \qquad \left. \mp \left\{ \cos(\pi/n_1) - \cos(\beta_a/n_1) \right\}^{-1} \right], \quad \phi \leqslant \dfrac{\pi}{2} - \dfrac{\beta_a}{2} \\[10pt] 0, \qquad \phi > \dfrac{\pi}{2} - \beta_a/2 \end{cases}$$

$$\tag{4}$$

$$\sqrt{\sigma_4} = \begin{cases} \dfrac{\sin(\pi/n_2)}{n_2} \sqrt{\dfrac{a_2 \csc\phi}{k \cos(\beta_a/2)}} \left[\left\{ \cos(\pi/n_2) - \cos\left(\dfrac{3\pi+2\phi}{n_2}\right) \right\}^{-1} \right. \\ \qquad \left. \mp \left\{ \cos(\pi/n_2) - \cos(\beta_a/n_2) \right\}^{-1} \right], \quad \phi \leqslant \alpha - \beta_a/2 \\[10pt] 0, \quad \pi/2 + \beta_a/2 > \phi > \alpha - \beta_a/2 \\[10pt] \dfrac{\sin(\pi/n_2)}{n_2} \sqrt{\dfrac{a_2 \csc\phi}{k \cos(\beta_a/2)}} \left[\left\{ \cos(\pi/n_2) - \cos\left(\dfrac{-\pi+2\phi}{n_2}\right) \right\}^{-1} \right. \\ \qquad \left. \mp \left\{ \cos(\pi/n_2) - \cos(\beta_a/2) \right\}^{-1} \right], \quad \phi \leqslant \dfrac{\pi}{2} + \dfrac{\beta_a}{2} \end{cases}$$

$$\tag{5}$$

And the phase referenced to the base of the frustum are given by:

$$\rho_1 = -2k\cos\left(\beta a/2\right)\left[a_1\sin\phi + 2h\cos\phi\right] + \pi/4$$

$$\rho_2 = -2k\,a_2\sin\phi\,\cos\left(\beta a/2\right) + \pi/4$$

$$\rho_3 = +2k\cos\left(\beta a/2\right)\left[a_1\sin\phi - 2h\cos\phi\right] - \pi/4$$

$$\rho_4 = +2k\,a_2\sin\phi\,\cos\left(\beta a/2\right) - \pi/4$$

where α is the frustum angle in radians.

$$\alpha = \tan^{-1}\left(\frac{a_2 - a_1}{2h}\right)$$

$$\eta_1 = \frac{3}{2} - \frac{\alpha}{\pi}$$

$$\eta_2 = \frac{3}{2} + \frac{\alpha}{\pi}$$

$$k = 2\pi/\lambda$$

Upper sign in above equations correspond to vertical polarization and lower sign corresponds to horizontal polarization.

Also using small approximation, at and near the nose-on axial aspects, one obtains:

$$\sqrt{\sigma}\, e^{j\rho} = 2\sqrt{\pi}\left[\left(k\cos(\beta_a/2)\right)a_1^2 \; \frac{J_1(2ka_1\sin\phi\cos(\beta_a/2))}{(2ka_1\sin\phi\cos(\beta_a/2))} e^{-j\pi/2} \right.$$

$$\left. \pm\; a_1 \frac{\sin(\pi/\eta_1) J_2(2ka_1\sin\phi\cos(\beta_a/2))}{\eta_1(\cos(\pi/\eta_1) - \cos(\beta_a/\eta_1))}\right]\cdot \exp\left[-j4kh\cos\phi\cos\left(\frac{\beta_a}{2}\right)\right]$$

$$+\; 2\sqrt{\pi}\, a_2 \frac{\sin(\pi/\eta_2)}{\eta_2}\left[\frac{J_0(2ka_2\sin\phi\cos(\beta_a/2))}{\cos(\pi/\eta_2) - \cos(3\pi/\eta_2)}\right.$$

$$-j\,\frac{2\sin(3\pi/\eta_2)\tan\phi}{\eta_2}\cdot \frac{J_1(2ka_2\sin\phi\cos(\beta_a/2))}{(\cos(\pi/\eta_2) - \cos(3\pi/\eta_2))^2}$$

$$\left. \pm\; \frac{J_2(2ka_2\sin\phi\cos(\beta_a/2))}{(\cos(\pi/\eta_2) - \cos(\beta_a/\eta_2))}\right]$$

At and near the tail-on aspect ($\phi = \pi$) small angle approximation of equations (2)-(5) yield:

$$\sqrt{\sigma}\, e^{j\rho} = 2\sqrt{\pi}\left[\left(k\cos(\beta_a/2)\right)a_2^2 \; \frac{J_1(2ka_2\sin\phi\cos(\beta_a/2))}{(2ka_2\sin\phi\cos(\beta_a/2))} e^{-j\pi/2} \right.$$

$$\left. \pm\; a_2 \frac{\sin(\pi/\eta_2)}{\eta_2} \frac{J_2(2ka_2\sin\phi\cos\beta_a/2)}{(\cos(\pi/\eta_2) - \cos(\beta_a/\eta_2))}\right]$$

For $\bar{\Phi} = \pi/2 - \alpha$, the expression for the radar-cross-section, using physical optics theory, may be written as:

$$\sigma(\phi = \pi/2 - \alpha) = \frac{8\pi}{9\lambda} \left[a_2^{3/2} - a_1^{3/2} \right]^2 \cos(\beta_a/2) \Big/ \left[\sin^2\alpha \cos\alpha \right]$$

EXPERIMENTAL DETAILS

The experiment was conducted by General Dynamics at Forth Worth, Texas. Operating frequency of $6 \cdot 050$ GHz was used. All other details are listed in the respective diagrams.

ANALYTICAL AND/OR EXPERIMENTAL PLOTS

These results are ploted in Figs. 2 and 3.

INTERPRETATION OF RESULTS

The general agreement between theory and experiment is very good. Generalization of formulas in terms of an unrestricted bistatic parameter β (where β is the projection of β in the azimuth plane) is straight forwarded. Therefore, the theory is suitable for scintillation, doppler spectrum and coherent radar studies, as well as for grosser aspects of RCS investigations.
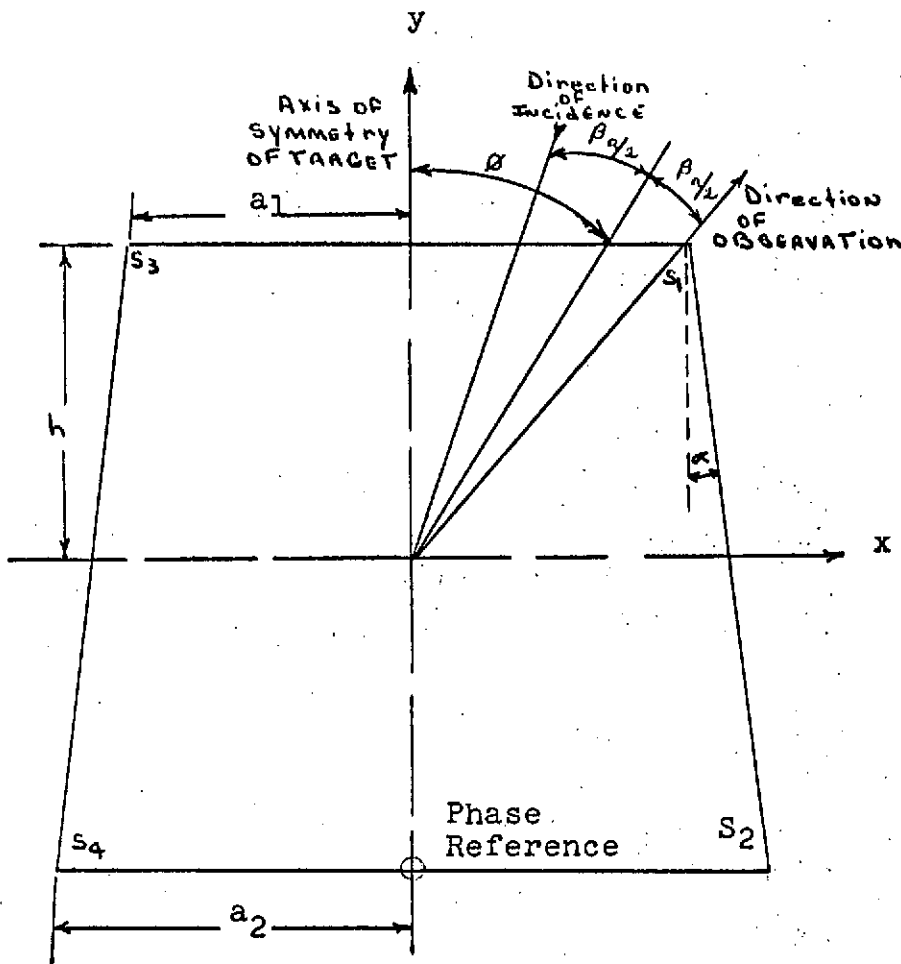
Fig. 1. Scattering centers on frustrum.

Aspect Angle ⌀ degrees

Aspect Angle ⌀ degrees
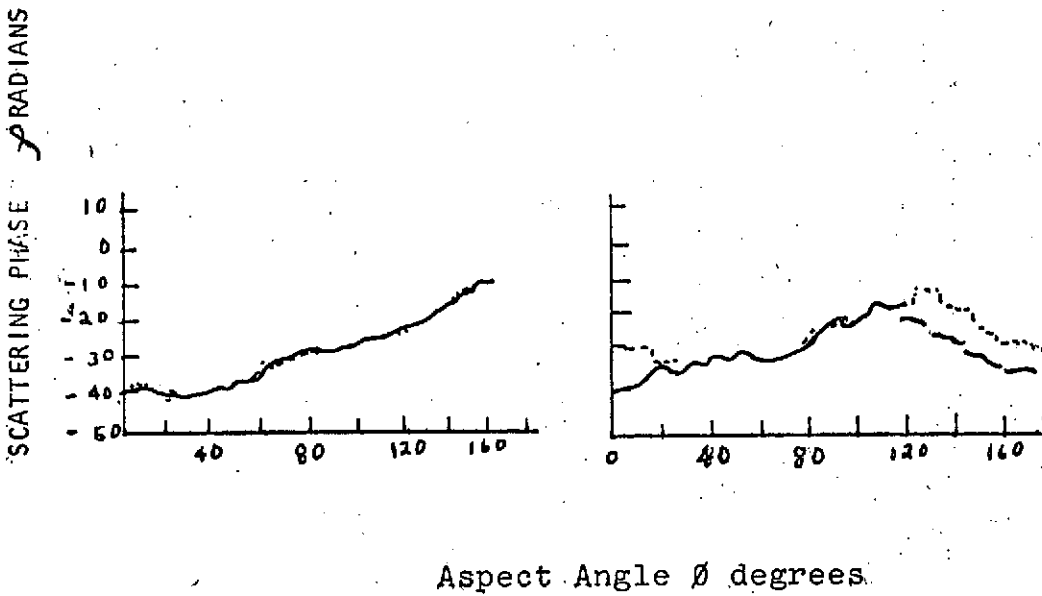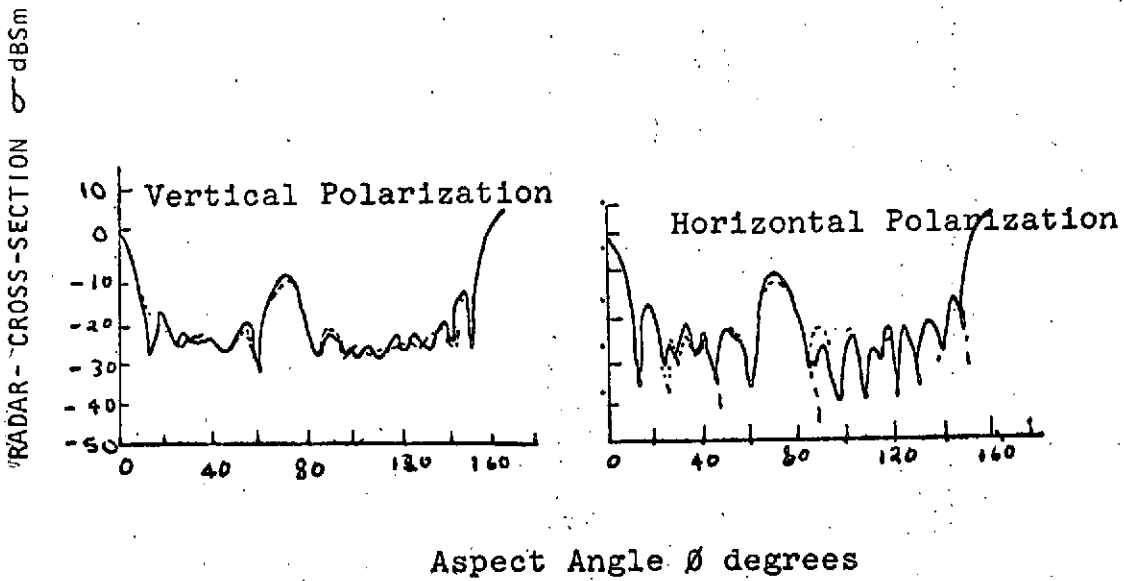
Fig.2. Bistatic scattering matrix for frustrum. $2a_1=2.507$,
$2a_2=3.239$, $2h=2.083$, β_q =30.0 degrees. Dotted line
indicates geometrical diffraction theory (single diffraction);
solid line indicates experimental.
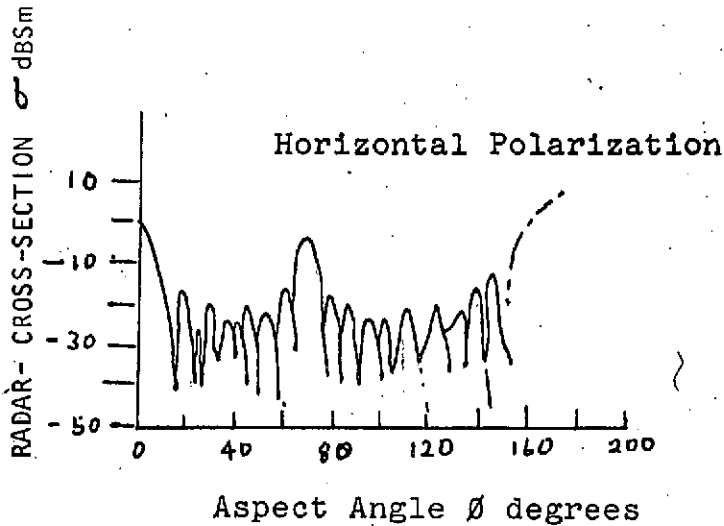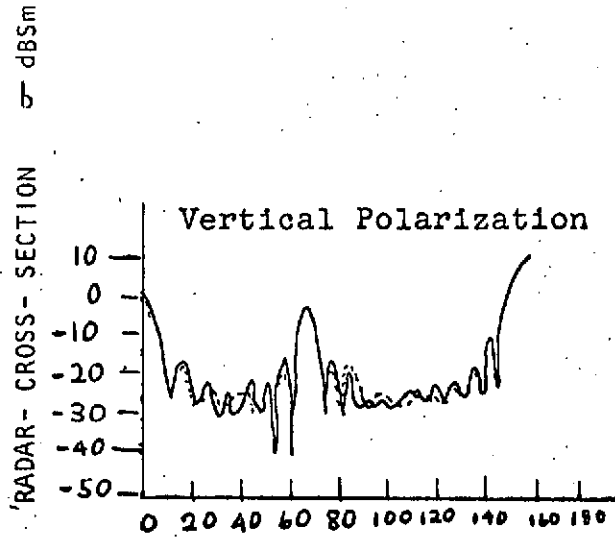
Fig.3. Bistatic radar cross section of frustrum for vertical and horizontal polarizations. $2a_1=2.510$, $2a_2=3.844$, $2h=3.804$, $\phi_o=30.0$ degrees. Dotted line indicates geometrical diffraction theory (single diffraction); solid line indicates experimental.

RADAR-CROSS-SECTION OF A FINITE RECTANGULAR CYLINDER

Keller's Geometrical Theory of Diffraction, with scattering centers concept, is applied to investigate the high frequency scattering from a finite rectangular cylinder. Theoretical expressions of RCS as a function of frequency and aspect angle are derived. Experimental work is also reported to compare the results for the mono-static case.

TARGET AND COORDINATE SYSTEM

The target geometry and coordinate system used is shown in Fig. 1.

ANALYTICAL EXPRESSIONS

Based upon this theory, there will be three scattering centers and the final expression for the mono-static radar-cross-section may be written as:

$$\sigma = \left[\sqrt{\sigma_1} \, exp \, j\beta_1 + \sqrt{\sigma_2} \, exp \, j\beta_2 + \sqrt{\sigma_3} \, exp \, j\beta_3 \right]^2$$

with the amplitude of the contribution reradiated from each center given by

$$\sqrt{\sigma_1} = \frac{4b}{3\sqrt{\pi}} \sin\left(\tfrac{2\pi}{3}\right) \left[\left\{ \cos\left(\tfrac{2\pi}{3}\right) - \cos\left(\tfrac{2}{3}\pi + \tfrac{4}{3}\phi\right) \right\}^{-1} \right.$$
$$\left. \mp \left\{ \cos\left(\tfrac{2\pi}{3}\right) - 1 \right\}^{-1} \right]$$

$$\sqrt{\sigma_2} = \frac{4b}{3\sqrt{\pi}} \sin\left(\frac{2\pi}{3}\right) \left[\left\{ \cos\left(\frac{2\pi}{3}\right) - \cos\left(\frac{4\phi}{3}\right) \right\}^{-1} \right.$$

$$\left. \mp \left\{ \cos\left(\frac{2\pi}{3}\right) - 1 \right\}^{-1} \right]$$

$$\sqrt{\sigma_3} = \frac{4b}{3\sqrt{\pi}} \sin\left(\frac{2\pi}{3}\right) \left[\left\{ \cos\left(\frac{2\pi}{3}\right) - \cos\frac{2}{3}(\pi - 2\phi) \right\}^{-1} \right.$$

$$\left. \mp \left\{ \cos\left(\frac{2\pi}{3}\right) - 1 \right\} \right]$$

and with the phase of contrubution reradiated from each center given by:

$$f_1 = -2k(a \sin\phi + c \cos\phi) + \pi/4$$

$$f_2 = -2k(a \sin\phi - c \cos\phi) + \pi/4$$

$$f_3 = 2k(a \sin\phi - c \cos\phi) + \pi/4$$

$k = 2\pi/\lambda$: λ = wavelength.

These equations were programmed on computer for $0.5° \leq \phi \leq 89.5°$

EXPERIMENTAL DETAILS

Experiment was conducted at Cornell Aeronautical Labs, to measure the mono-static radar-cross-section of the rectangular cylinder using ka band pulsed-radar range with operating frequency 34.85 GHz. The model dimensions used are: $2a = 14.763\lambda$; $2b = 171716\lambda$; $2c = 2.26\lambda$.

ANALYTICAL AND/OR EXPERIMENTAL PLOTS

The results are plotted in Figs. 2a and 2b.

INTERPRETATION OF RESULTS

There seems to be a good agreement at all aspect angles in both cases between theory and experiment. It will improve for long cylinders and when the effect of multiple diffractions terms are also taken into account. The present analysis can be extended to handle bistatic and specular cases. The espressions valid for arbitrary aspect angles are yet to be develpoed.
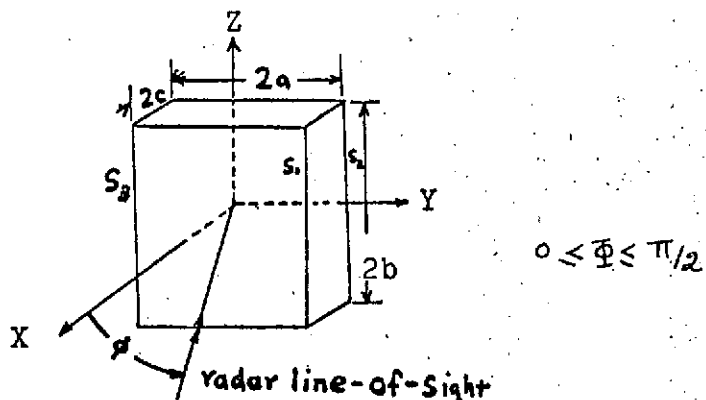
Fig. 1 Scattering centres on a rectangular cylinder.

a , Horizontal-Polarization

b Vertical-Polarization
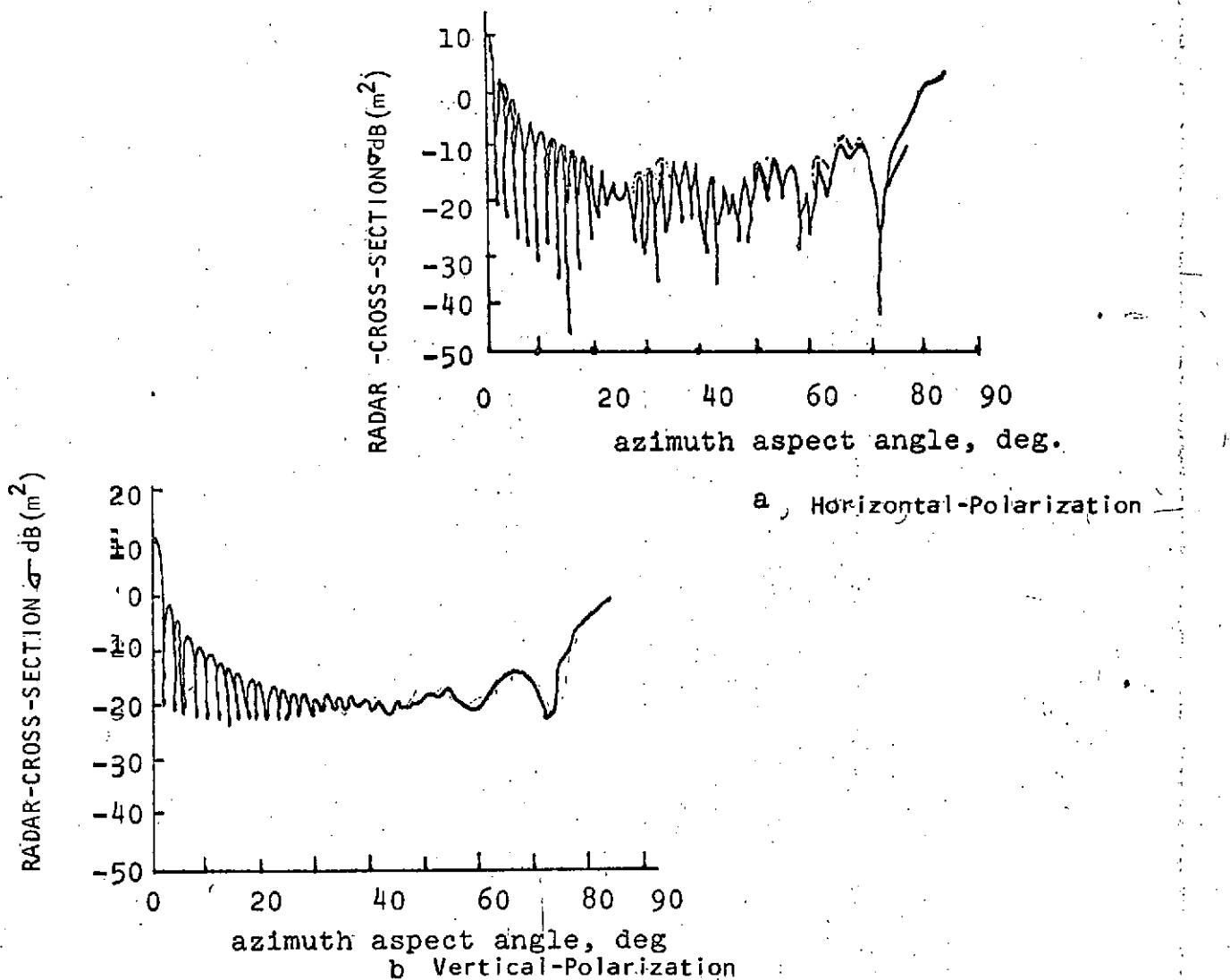
Fig. 2 Radar cross-section of rectangular cylinder for
vertical and horizonital polarisations.

Experimental   Theoretical (Single-diffraction
                                    terms only)

RADAR SCATTERING FROM BLUNTED CONE TIPS

In this study radar-cross-section expressions are developed by using exact electromagnetic theory for:

1. Ball-point tip cone
2. Round-tip cone
3. Concave-tip cone

Results obtained from these expressions are further compared with the results obtained by Physical Optics Theory and the so called "Crude Model Theory," which approximates blunt cone as a combination of pointed cone plus sphere.

TARGET AND COORDINATE SYSTEM

1. Ball-point tip semi-infinite cone is shown in Fig. 1a.

   where $r = a$ for $0 \leqslant \theta \leqslant \pi - \alpha$

   $\theta = \pi - \alpha$ for $\lambda > a$

2. Round-tip semi-infinite cone is shown in Fig. 1b.

   where $r = -R \sec \alpha [\cos \theta + \sqrt{\cos^2 \theta - \cos^2 \alpha}]$

   for

   $R = a \cot \alpha$

3. Concave-tip semi-infinite cone is shown in Fig. 1c.

   where $r = R$ for $\pi - \alpha \leqslant \theta \leqslant \pi$

ANALYTICAL EXPRESSIONS

1. Using exact theory, the radar-cross-section of a ball-point tip cone may be written as:

$$\sigma = \pi/k^2 \left| \left[\sum_{\gamma} \frac{\gamma(\gamma+1)}{N_\gamma} \exp(j\gamma\pi) - \sum_{\mu} \frac{\mu(\mu+1)}{N_\mu} \exp(j\mu\pi) \right] \right.$$

$$\left. - 2j \left[\sum_{\gamma} \frac{\gamma(\gamma+1)}{N_\gamma} \exp(j\gamma\pi) \frac{J_\gamma/n_\gamma}{1+jJ_\gamma/n_\gamma} - \sum_{\mu} \frac{\mu(\mu+1)}{N_\mu} \exp(j\mu\pi) \frac{J_\mu^*/n_\mu^*}{1+jJ_\mu^*/n_\mu^*} \right] \right|^2$$

$$\gamma_n \approx n - \frac{n(n+1)}{4} \alpha^2 + \left\{ n^2(n+1)^2 \left[1 + \Im m(\alpha/2) + \psi(n+1) \right. \right.$$
$$\left. + \psi(n-1) - 2\psi(1) \right] + 2n(n+1)^3 + 4n(n+1)/3 + 3(n-1)+$$
$$\left. n(n+1)(n+2)/2 \right\} \alpha^4/16$$

$$\mu_n \approx n + \frac{n(n+1)}{4} \alpha^2 + \left\{ n^2(n+1)^2 \left[1 + 2\ln(\alpha/2) + \psi(n+1) \right. \right.$$
$$\left. + \psi(n-1) - 2\psi(1) \right] + n(n+1)(2n+1) - n(n-1)(n+1)*$$
$$\left. (n+2)/2 - n(n+1)/3 \right\} \alpha^4/16$$

$$\begin{bmatrix} N_{\gamma_n} \\ N_{\mu_n} \end{bmatrix} = 2n(n+1)/2n+1 \left\{ 1 \pm \alpha^2 2n(n+1)/2(2n+1) \right\}$$

These approximations are valid, provided that $n\alpha << 2$

11. Using exact theory, radar-cross-section expressions for a round-tip and concave-tip cones may be written as:

$$\sigma = \pi/k^2 \left| \alpha^2/2 - 2j \sum_{n,m} j^{m+n} (2m+1) n(n+1)/m(m+1) \times \right.$$
$$\left. \left[\frac{A_{n,\gamma_m} - j C_{n,\mu_m}}{B_{n,\gamma_n}} - \frac{C_{n,k_m} + j \ddot{A}_{n,\gamma_m}}{D_{n,\mu_n}} \right] \right|^2$$

III. Using physical optics theory, for nose-on incidences, the back-scattering cross-section for the concave tip is: (neglecting the cone termination at infinity)

$$\sigma = 4\pi k^2 R^4 \left| \frac{(2jkR-1)\exp(2jkR)}{(2kR)^2} - \frac{(2jkR\cos\alpha-1)\exp(2jkR\cos\alpha)}{(2kR\cos\alpha)^2} \right|^2$$

IV. Using physical optics theory, the backscattering-cross section may be written as:

$$\sigma = \pi a^2 \left\{ 1 - \frac{\sin[2ka(1-\sin\alpha)]}{ka\cos^2\alpha} + \frac{1+\cos^4\alpha}{4(ka)^2\cos^4\alpha} - \frac{\cos[2ka(1-\sin\alpha)]}{2(ka)^2\cos^2\alpha} \right\}$$

V. RCS for round-tip cone, using crude model, may be written as:

$$\sigma = \sigma_{cone} + \sigma_{sphere}$$

Futhermore, Table 1 shows scaling of ($\sigma/\pi a^2$) min. as a function of α .

TABLE 1

Scaling of $(\sigma/\pi a^2)_{min}$ As a Function of α

Tip Shape		$(\sigma/\pi a^2)_{min}$	Location (ka)
Rounded	Exact	$0.7\,\alpha^2$	$0.8\,\alpha$
	Physical Optics	$0.8\,\alpha^2$	$0.8\,\alpha$
Concave	Exact	$0.6\,\alpha^2$	$0.9\,\alpha$
	Physical Optics	α^2	$0.75\,\alpha$
Ball-Point	Exact	$1.6\,\alpha^{8/3}$	$0.5\,\alpha^{2/3}$
	Crude Model	$1.6\,\alpha^{8/3}$	$0.5\,\alpha^{2/3}$

ANALYTICAL AND/OR EXPERIMENTAL PLOTS

The above equations are programmed on a computer and results are plotted in Figures 2, 3, 4, and 5.

INTERPRETATION OF RESULTS

For the ball-point tip case, exact theory agrees very closely with the crude model (σ = σ cone + σ sphere) results. The RCS of rounded and concave tips were calculated by means of exact theory and by using physical optics theory. These results show close agreement. The agreement is better for the rounded tip is probably due to the smooth tip cone join, wereas crude model failed miserably in cases of round and concave tip cones.
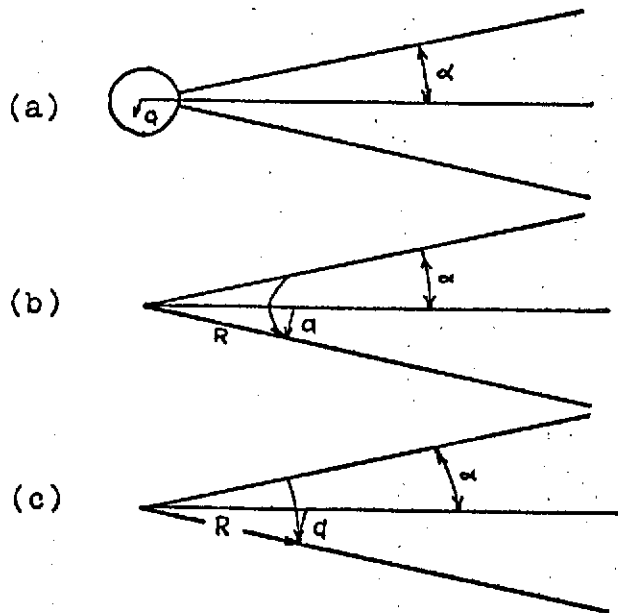
Fig. 1. (a) Ball-point tip. (b) Rounded tip. (c) Concave tip.
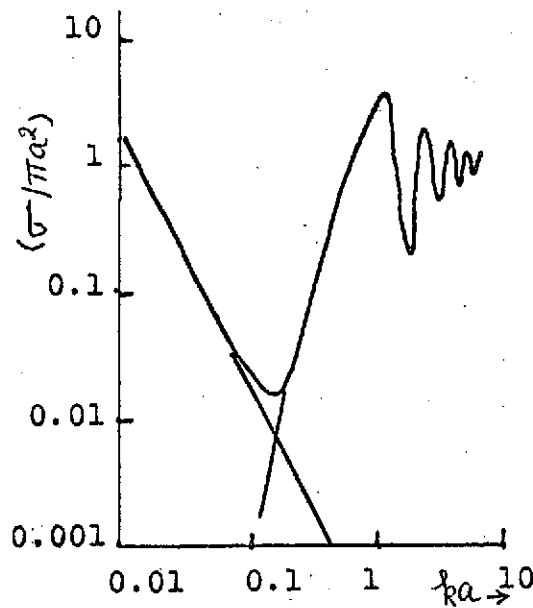
Fig. 2. $\sigma/\pi a^2$ for ball-point tip as a function of ka for $\alpha = 10°$; also shown lightly are the curves for a pointed cone and an isolated sphere.

Fig. 3. $(\sigma/\pi a^2)$ for ball-point tip as a function of ka for α =5°, 8°, 10°, and 12°; curves for pointed cones and an isolated sphere are shown lightly.

Fig. 4. $\sigma/\pi a^2$ for concave and rounded tips as functions of ka for α =10°; also shown are physical optics results.

Fig. 5. $\sigma/\pi a^2$ for rounded tip as a function of ka for α =5°, 8°, 10°, and 12°.

RADAR CROSS SECTION OF SPHERICAL SHELL SEGMENTS

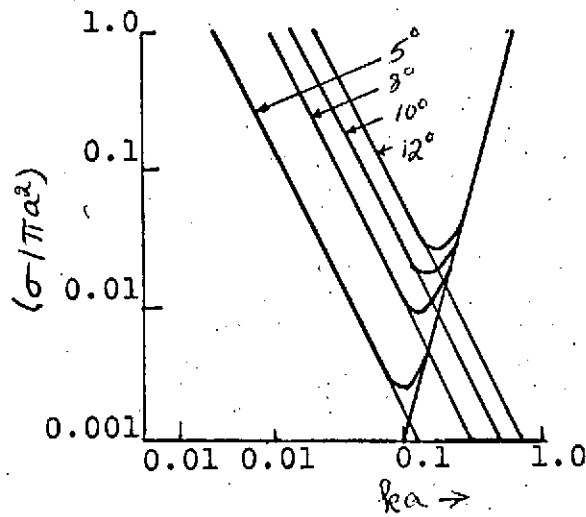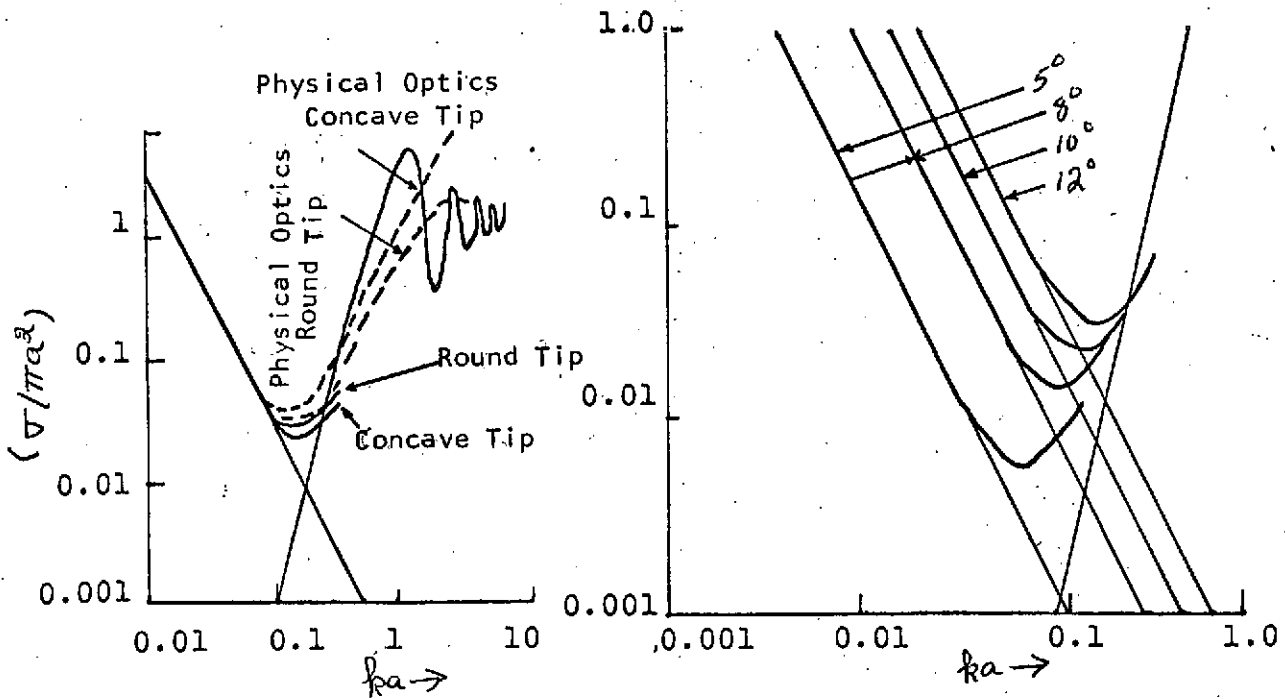This study derives the far-field backscatter radar cross section of a spherical shell for nose-on and near nose-on aspects for the high frequency case. The theoretical expressions are derived by first computing specular contributions by physical optics method and then adding to it the edge diffracted term. The sommerfield half-plane solution is modified to give the edge contribution. This technique involves deriving a correction factor, based on phase considerations, which takes into account the differences between the basic two dimensional problem considered and the three dimensional problem of interest here. Analytical results are compared with the experimental results.

TARGET GEOMETRY AND COORDINATE SYSTEM

The target geometry and coordinate system used is shown in Figs. 1, 2, and 4.

ANALYTICAL EXPRESSION

Using technique of adding specular terms by physical optics and the edge diffraction term by sommerfield theory; the expression for the RCS, for the nose-on case, may be written as:

$$\sigma = 4\pi a^2 \sin^2 ka\,(1 - \cos\gamma)$$

For the case of a near nose-on aspects, or in a region such that $\sin\theta \gg \dfrac{1}{2\,kb}$ (where $b = 1\,\sin\gamma$, $\theta < \gamma$). Furthermore, this region is characterized by the following:

1. Specular reflection is present.
2. All of the edge is in "lit" region.
3. The entire edge is not in phase at any angle.

RCS is given by:

$$\sigma\begin{pmatrix} V \\ H \end{pmatrix} = \pi a^2 \left| 1 - \sqrt{\sin\gamma/4\pi\,ka\sin\theta} \cdot \left\{ e^{j\eta_1}\left[\frac{1}{\sin(\gamma-\theta)} \mp 1\right] + e^{j\eta_2}\left[\frac{1}{\sin(\gamma-\theta)} \mp 1\right]\right\} \right|^2$$

where

$$\eta_1 = 2ka\left[1 - \cos(\gamma-\theta)\right] + \pi/4$$

$$\eta_2 = 2ka\left[1 - \cos(\gamma+\theta)\right] - \pi/4$$

EXPERIMENTAL DETAILS

To compare the theoretical results for nose-on case, experimental data obtained by Blore and Musal (1960 is used. But for the case of near-nose-on aspect, two models are made from this walled copper and measured at the Conduction Corpotation Radar Cross Section Measuring Range. Measurements were made at frequencies of 9.00 KMC and 10.23 KMC, and for both horzontal and vertical polarizations.

TABLE 1

Dimensions of Models

Model	Radius of Curvature (a)	γ	Ring Radius (b)
A	4.44 cm	$48\frac{1}{2}^{\circ}$	3.32 cm
B	4.44 cm	$60\frac{1}{2}^{\circ}$	3.87 cm

ANALYTICAL AND/OR EXPERIMENTAL PLOTS

Theoretical and experimental results for both cases are shown in Figures 2, 5, 6, 7, and 8.

INTERPRETATION OF RESULTS

It may be seen that results obtained are valid when $kb \gg 1$ (where b is the edge radius), for segments smaller than a hemisphere. For nose-on incidence, it is shown that the edge contribution has the same value as the well known specular contribution. An important consequence of this is strong interferences between these two contributors. Comparasion of this result with experiment shows that it is in good agreement. It is found to be much more accurate than the ordinary physical optics results.
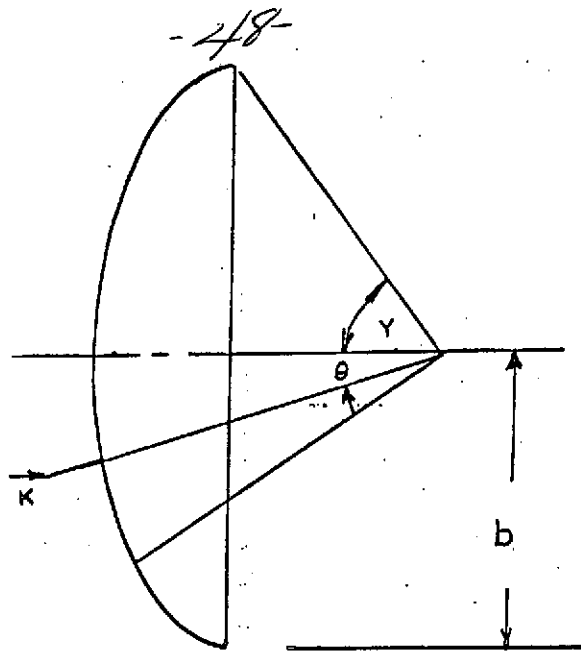
Fig. 1. Spherical shell segment.
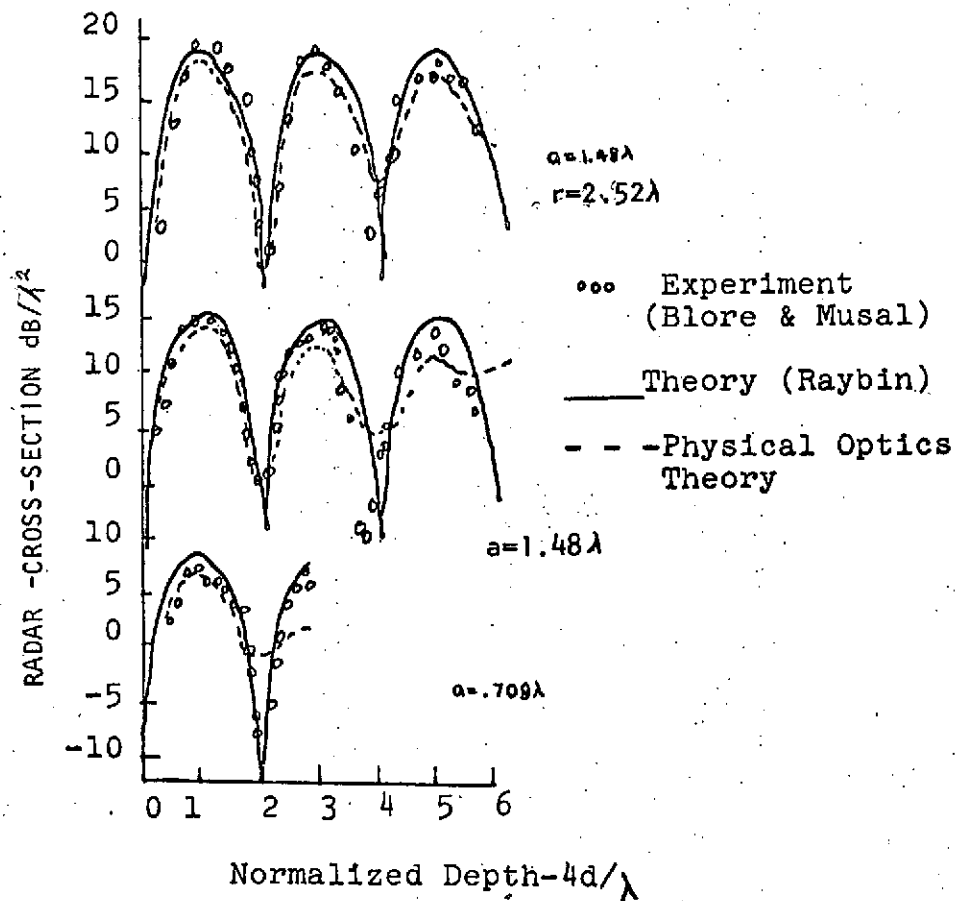
Fig.2. Radar cross section vs. depth for
spherical shell segment.
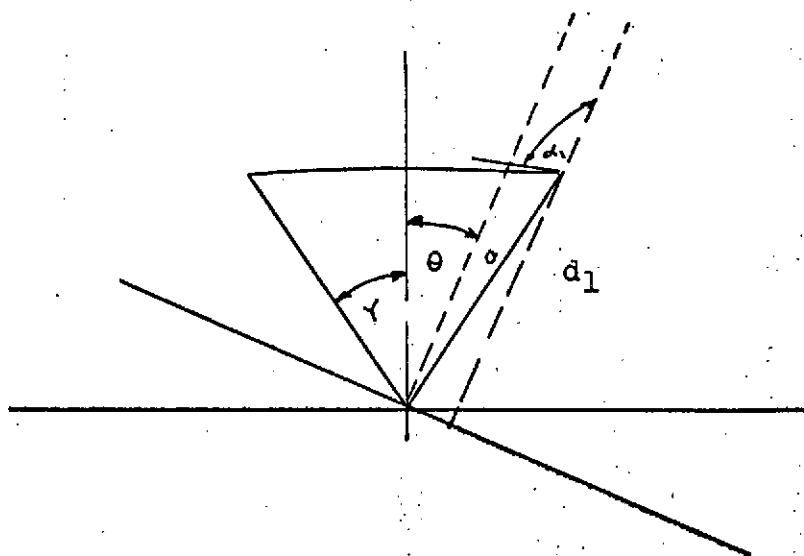
Fig. 3. Parameters for $\phi' = \phi$.
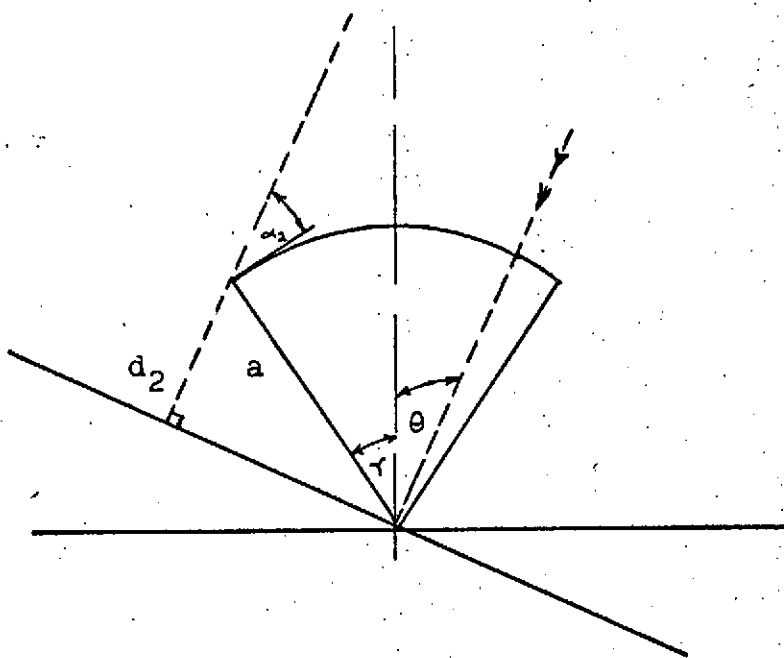
Fig. 4. Parameters for $\phi' = \phi + \pi$.

Horizontal Polarization

Vertical Polarization
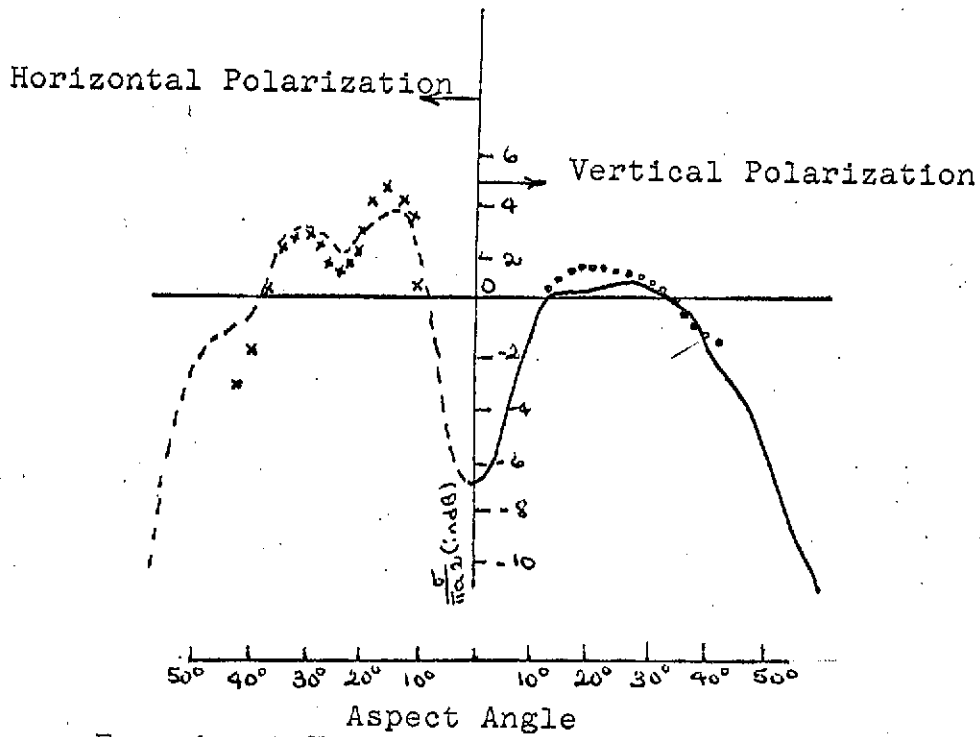
Aspect Angle

- - -Experiment-Hor. Pol.   Experiment-Ver. Pol.
x x xTheory -Hor. Pol.   ● ● ● Theory -Ver. Pol.

Fig.7. Cross section vs. aspect angle-Model A,
frequency =10.23 kMc.
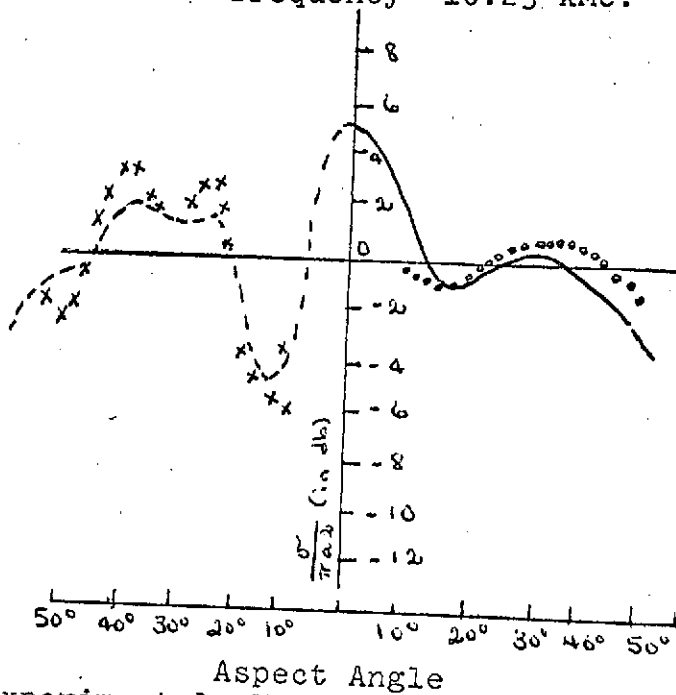
Aspect Angle

- - -Experimental -Hor. Pol.
x x xTheory -Hor. Pol.   Experimental -Ver. Pol.
                               Theory -Ver. Pol.

Fig.8. Cross section vs. aspect angle-Model B,
frequency =10.23 kMc.

Horizontal Polarization ←   → Vertical Polarization

Aspect Angle

x̄ x̄ x̄ x̄ Theory -Hor. Pol.   Experiment-Hor. Pol.   Experiment-Ver. Pol.   Theory -Ver. Pol.

Fig. 5. Cross section vs. aspect angle-Model A,
frequency =9.00 kMc.

Aspect Angle

x̄ x̄ x̄ x̄ Theory -Hor. Pol.   Experiment -Hor. Pol.   Experiment -Ver. Pol.   Theory -Ver. Pol.

Fig.6. Cross section vs. aspect angle-Model B,
frequency =9.00 kMc.

-51-

APPROXIMATIONS FOR DIELECTRIC OR PLASMA SCATTERERS

The study deals with the calculations of radar-cross-section of non-conducting bodies. Two approximate methods are proposed: The method of super-position approximation, for calculating the RCS of a concentric dielectric-clod sphere. This approximation treats scattering by outer and inner bodies separately; refraction at the free s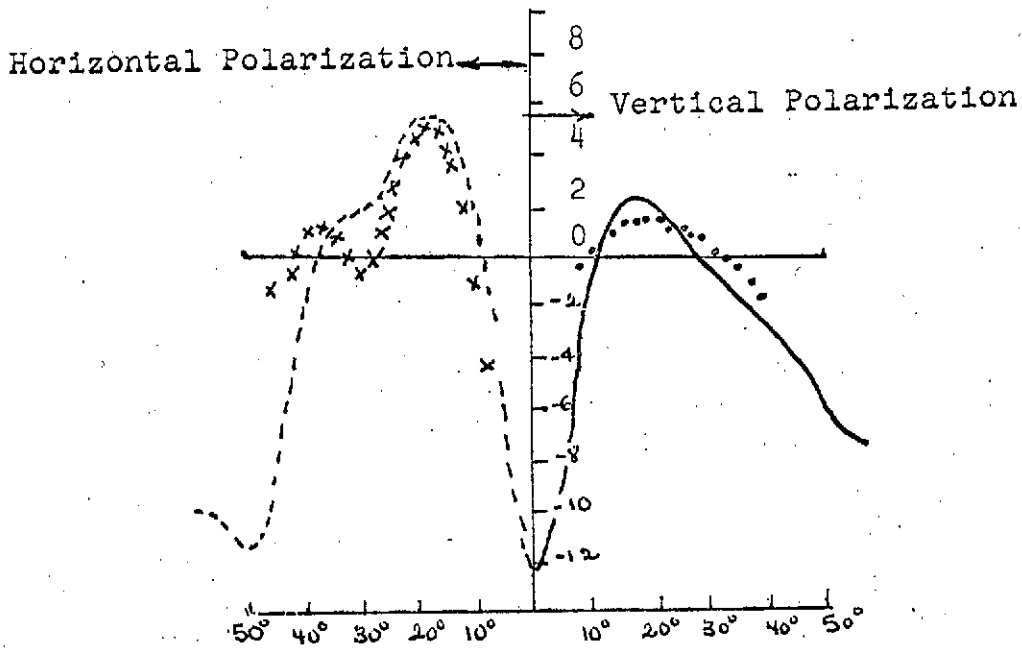pace/dielectric interface are introduces to modify the size of the inner body. This technique is easily applicable but requires that the properties of inner and outer body be known separately. This technique valid prococircled

$$(r_2 - r_1)/\lambda \; > \; (\lambda/4\pi n_1)$$

where r_1 r_2 are the radii of inner and outer shells.

Second technique called, "the modified geometrical optics theory", is applied to calculate the RCS of dielectric bodies. The basis of this modified geometrical optics methods is ray tracing. The wave fronts, which are normal to the rays, can be determined by tracing individual paths for a number of rays adjacent to the stationary ray and glory ray.

Finally, results obtained by these two methods are compared against the results obtained by exact theory.

ANALYTICAL AND/OR EXPERIMENTAL RESULTS

Results obtained by Supperposition, Modified Geometric Theory, and exact theory, techniques are shown in Figures

1, 2, 3, 4, and 5.

INTERPRETATION OF RESULTS

The analysis shows that superposition gives excellent results when the radius of the conducting body is less than 0.5λ . This method fails to predict the depth of the nulls accurately for extremely deep nulls and for bodies with larger inner radius but predicts the maxima for such cases with reasonable accuracy. The modified geometrical optics theory should be used for larger inner bodies if the depth of the nulls is of interest. The results obtained from these studies seem to be in good agreement with theory.

Exact
Superposition Component
Inner Component
Outer Component

$E_r = 1.25$
$r_1 = 0.05\lambda$

$r_2 = 0.36\lambda$
E-plane-plattering

$Log_{10}(\sigma/\pi \hat{z}_2^2)$

$E_2 = 0.75$

$r_1 = 0.05\lambda$
$r_2 = 0.435\lambda$

E-plane scattering

$Log_{10}(\sigma/\pi \hat{z}_2^2)$

$Er = 1.25$

$r_1 = 0.05\lambda$
$r_2 = 0.36\lambda$

H-plane-scattering

$Log_{10}(\sigma/\pi \hat{z}_2^2)$

$E_r = 0.75$
$r_1^r = 0.05\lambda$

$r_2 = 0.135\lambda$

H-plane scattering

Bistatic Angle β in Degrees
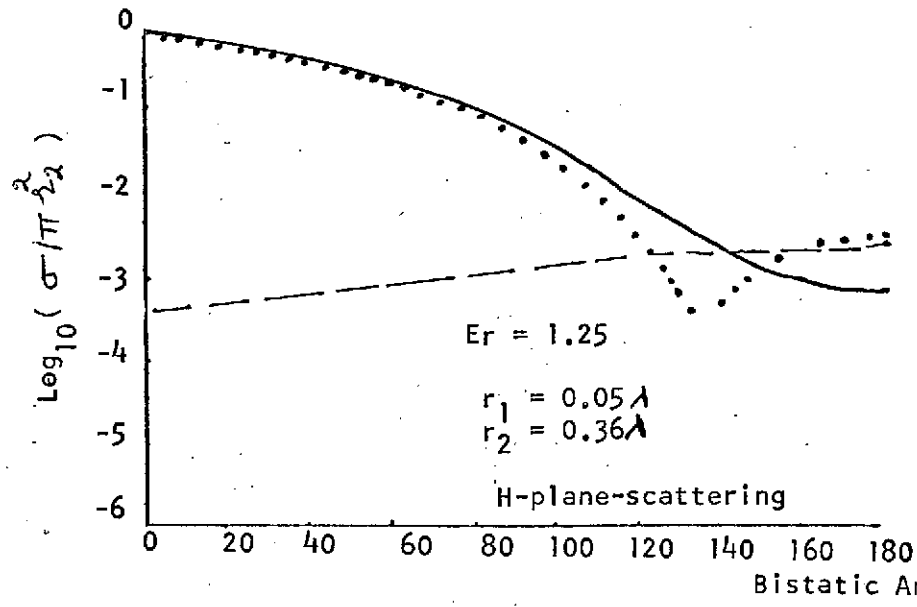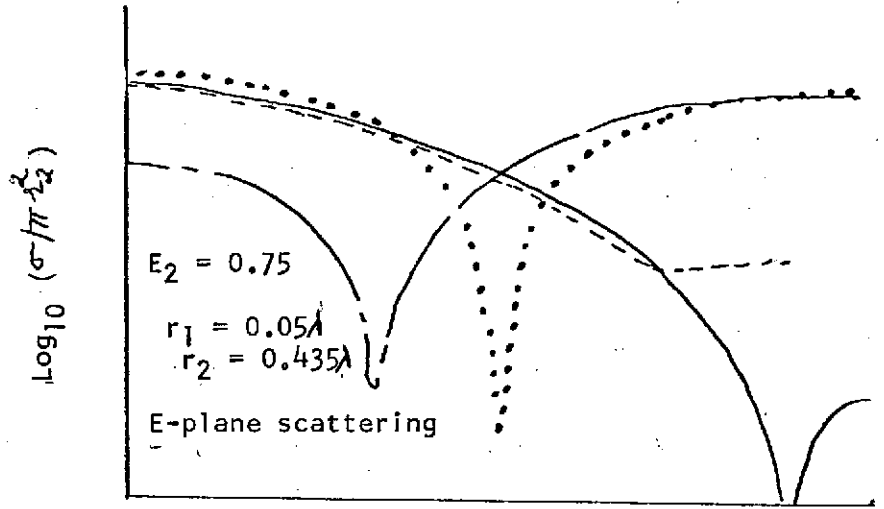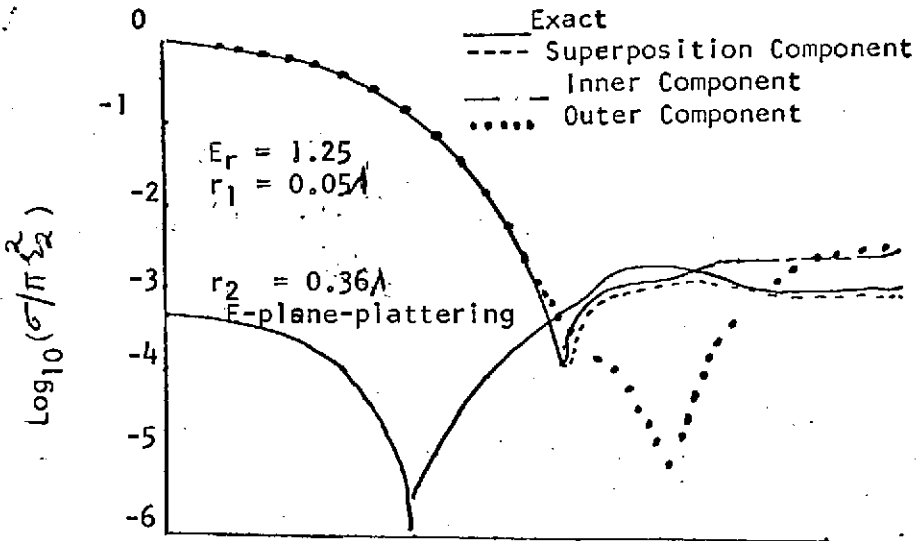
Fig. 1. Bistatic scattering of dielectric coated conducting spheres.
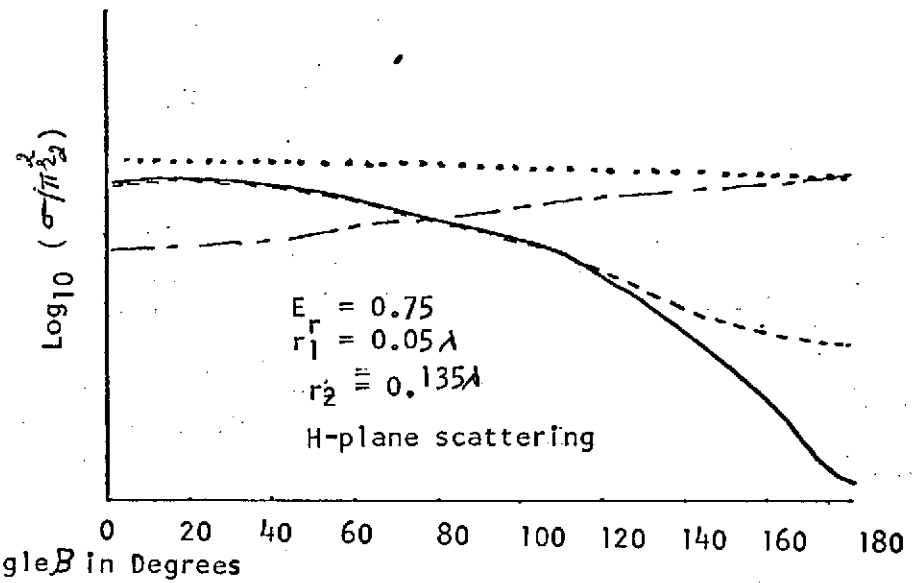
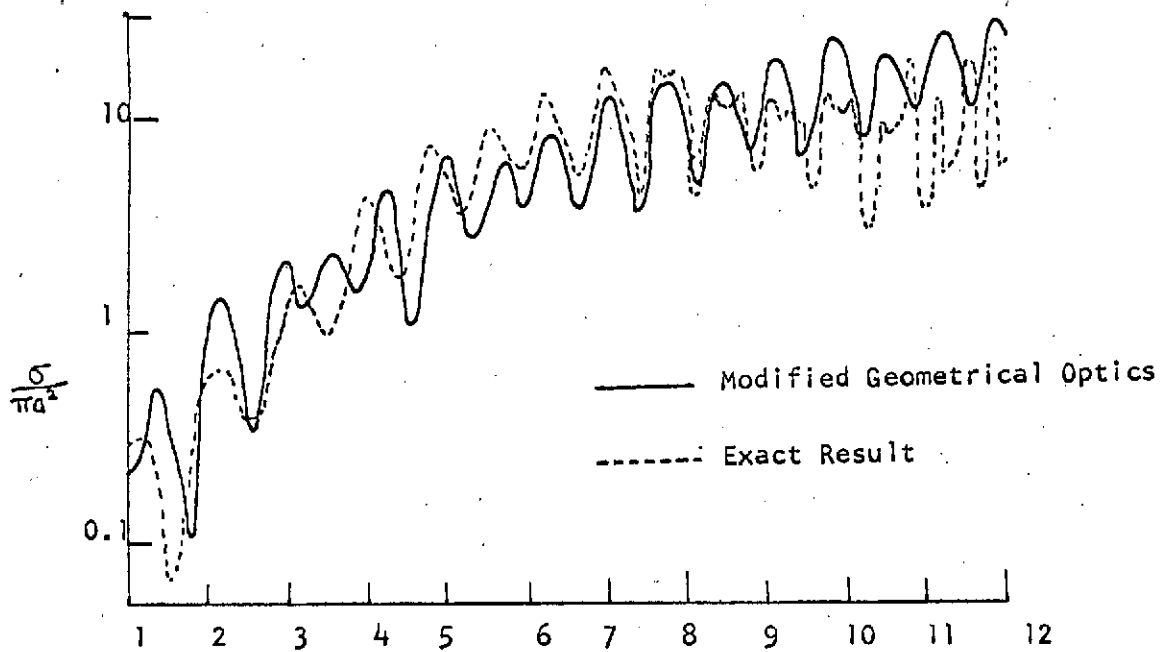Fig. 2. Bistatic scattering of dielectric coated conducting spheres.

Fig. 3. Baclscattering radar cross section of a dielectric sphere (E_2=2.592) as a function of ka by the use of modified geometrical optics.
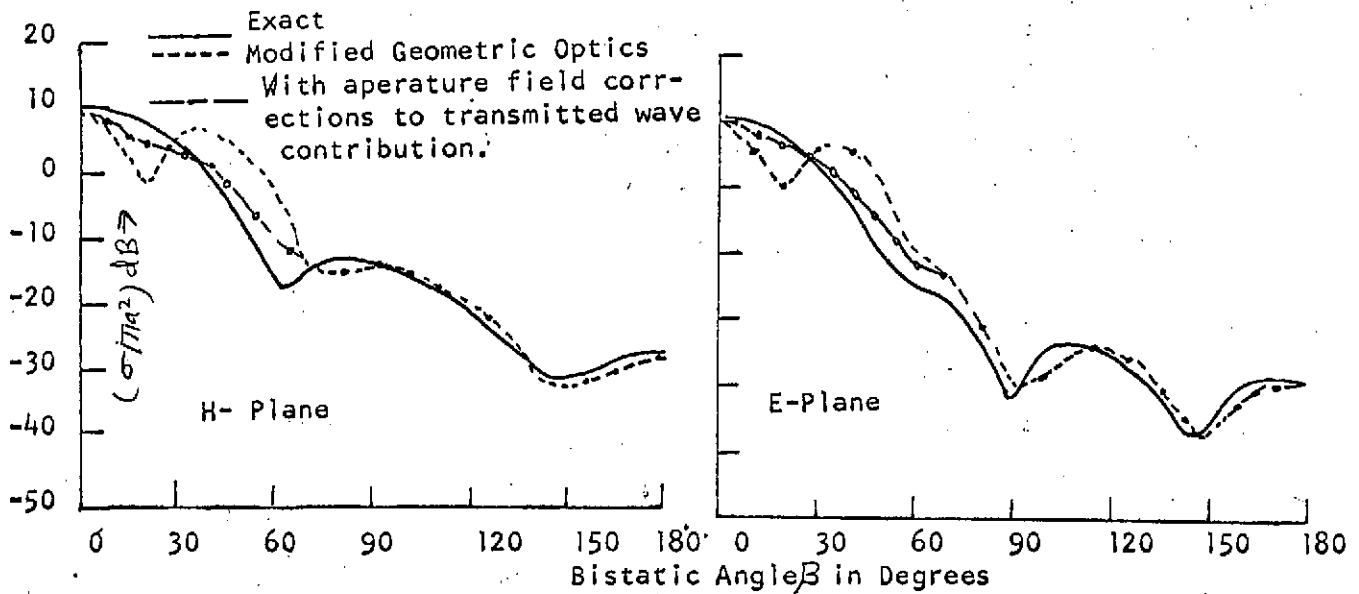
Fig. 4 Bistatic cross section of a plasma sphere with ϵ_r=0.74 and a/λ=0.75.
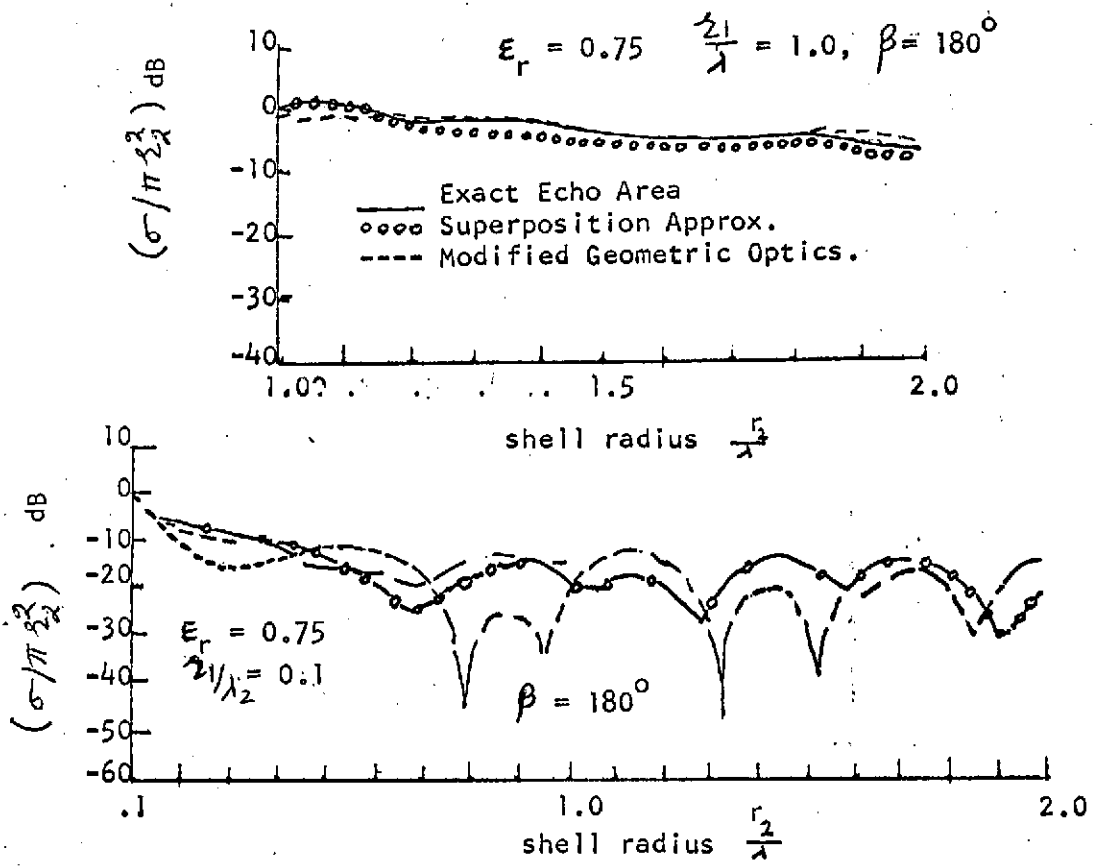
Fig. 5i. Radar cross sections of plasma-clad conducting spheres.

CROSS POLARIZATION DIAGNOSTICS

When a body is illuminated by an electromagnetic wave, the backscattered field usually includes direct and cross-polarization components. Historically, the former has been more widely studied because it is the component typically sensed by nomostatic radars and since it contains all specular contributions, it tends to be larger of the two. In contrast, the cross-polarized return is produced by more subtle contrubutions which elementary theories cannot predict.

Because of this depedence on the finer details of the object, the cross polarized return contains information about the scatter that is not readily obtainable from the direct return. The relationship of the transverse body dimensions and severity of any edges to the cross polarized RCS is shown.

ANALYTICAL EXPRESSIONS

Based upon geometrical theory of diffraction, for a right circular cone with half-angle γ , an expression for cross-polarized RCS (σ_{cr}) may be written as:

$$\frac{\sigma_{cr}}{\lambda^2} = \frac{1}{\pi} \left\{ A K a \, J_2(\xi) \right\}^2$$

where $A = n^{-1} \cot \pi /(2n)$; $n = \frac{3}{2} + \delta/\pi$, $\xi = 2 K_a \sin \phi$

and $J_2(\xi)$ is the bessel function of second order.

Equation 1 reduces to an expression for the disk for n = 2 but

is relatively insensitive to cone angle. Similarly, an expression

for a cone-sphere may be written as:

$$\frac{\sigma_{cr}}{\lambda^2} = \frac{1}{4\pi} \left\{ \frac{\cos^2 \gamma \cos \phi}{\cos 2\gamma + \cos 2\phi} \right\}^2 \left\{ J_2^2(\xi) + \tan^2 \gamma \tan^2 \phi \, J_1^2(\xi) \right\}$$

where $\xi = 2 ka \cos \gamma \sin \phi$; ϕ aspect angle.

EXPERIMENTAL DETAILS

The -S- and -X- band measurements of the backscattering for

four axially symmetric bodies: thin disks, right circular cones,

cones with rounded edges and cone-spheres, are undertaken. The

transmitted and received polarizations are inclined $\pm 45^o$ to the

horizontal, and the resulting patterns were recorded over an

angular range $-30^o \leqslant \phi \leqslant 30^o$ about the axis.

ANALYTICAL AND/OR EXPERIMENTAL PLOTS

The analytical and experimental results obtained are shown in

Fig. 1.

INTERPRETATION OF RESULTS

The analysis shows that disks and sharply edged cones have the strongest returns, cone-spheres the weakest, and cones with rounded edges have intermediate values. The difference between cones and cone-sphere is as much as 30dB for ka = 20. The agreement between theory and experiment is of the order of 1dB for disks and narrow cones. In case of cone-sphere, agreement with the experiment is reasonable in view of the extreme by low level measures, but the systematic discrepancy for small (ka) suggests that there may be another source of depolarization, such as creeping waves.
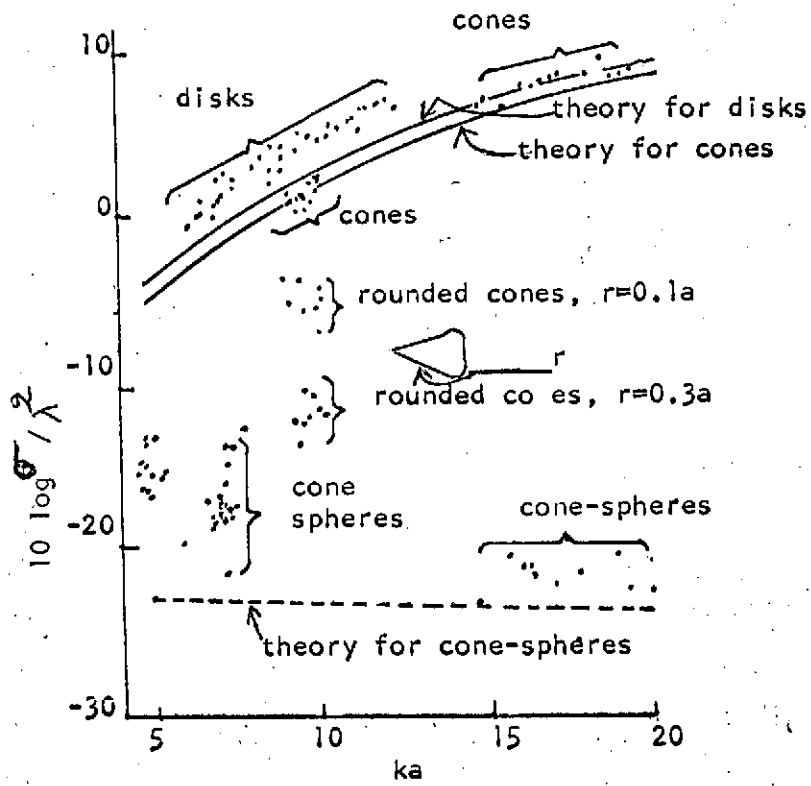
Fig. 1. Cross polarized radar cross sections.

THE BACKSCATTERING RADAR CROSS SECTION OF LONG THIN DIELECTRIC BODIES OF REVOLUTION ON A METAL PLANE

Approximate theoretical expressions are developed for a thin dielectrix body of revolution on a perfectly conduction plane and surrounded by free space. In particular cases of circular sylinder and cone are treated. The development is based upon image theory.

TARGET AND COORDINATE SYSTEM

The target and coordinate system is shown in Fig. 1.

ANALYTICAL EXPRESSIONS

Case 1- For the case of a circular cylinder, ρ = a, and the RCS expression may be written as:

$$\sigma \simeq k^4 V^2 (A \cos^2\alpha + B \sin^2\alpha) \tag{1}$$

where $k = 2\pi/\lambda$ is the free space wave number, $V = \pi \ell a^2$ is the volume of the cylinder, and

$$A = A(\epsilon, \beta) = \frac{\sin^4\beta}{\pi} \left(\frac{\epsilon-1}{\epsilon+1}\right)^2 \left\{(\epsilon+1)^2 + 4\epsilon^2 \cot^2\beta\right\} \tag{2}$$

$$B = B(\epsilon, \beta) = \frac{\sin^4\beta}{\pi} \left(\frac{\epsilon-1}{\epsilon+1}\right)^2 \left\{1 + \frac{\sin^2\beta}{\epsilon - \cos^2\beta}\right\}^2 \tag{3}$$

-64-

Equation (1) is valid if the following assumptions are made:

$$\frac{\ell}{\lambda} \gg 1 \tag{4}$$

$$k a \sqrt{(\epsilon - \cos^2 \beta)} \ll 1 \tag{5}$$

$$2 k \ell \cos \beta \gg 1 \tag{6}$$

$$\beta \text{ is bounded away from zero} \tag{7}$$

$$\sin \beta / \sqrt{(\epsilon - \cos^2 \beta)} \text{ is bounded away from zero} \tag{8}$$

Case 11- For the case of a right circular cone, whose lateral surface is defined as:

$$\beta = a (1 - (z/\ell)) \quad , \qquad 0 \leq z \leq \ell$$

$$\beta$$

$$a/\ell \ll 1$$

the RCS expressions are given by equations (1), (2), and (3), where now $V = \pi \ell a^2 / 3$, volume of cone. Assumptions (4) - (8) also apply in this case.

INTERPRETATION OF RESULTS

The expressions of RCS derived here are valid for all bodies of revolution satisfying the restrictions outlined and such that on their lateral surface $f = f(z)$:

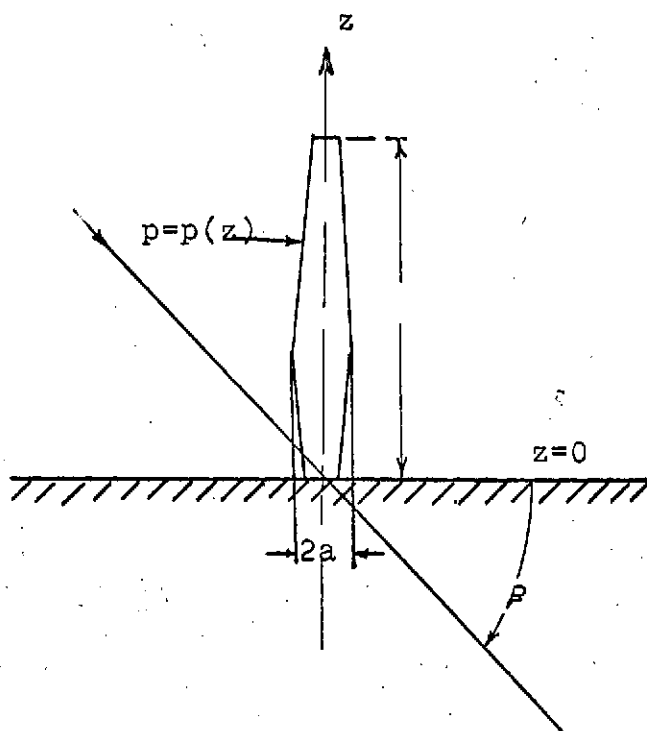$$\left| (df/dz) \right| \ll 1$$

$$\text{for } 0 \leq z \leq \ell$$

Fig. 1.   Geometry for the scattering problem.

PREDICTION OF RADAR CROSS SECTION OF A COMPOSITE TARGET USING SCATTERING CENTER THEORY

The radar-cross-section of a composite body consisting of sections of a sphere, cone, cylinder, flare and frustrum is predicted. The theoretical expressions predicted are programmed on a computer and the results are plotted. The cattering center concept is used and such a target will have eight scattering centers.

TARGET GEOMETRY COORDINATE SYSTEM

The target geometry and coordinate system used is shown in Figures 1 and 2.

ANALYTICAL EXPRESSIONS

A detailed derviation of scattering center contributions is not required for the composite body. Using Geometrical theory of diffraction, one may write by inspection

$$\sqrt{\sigma_2} = \frac{\sin \pi/n_2}{n_2} \sqrt{\frac{a_1 \csc \phi}{k}} \left\{ \left[\cos \frac{\pi}{n_2} - \cos \frac{2\pi - 2\phi}{n_2} \right]^{-1} \mp \left[\cos \frac{\pi}{n_2} - 1 \right]^{-1} \right\}$$
$$0 \leq \Phi \leq \Phi_2$$

$$= 0 \; ; \; \Phi > \Phi_2$$

$$\sqrt{\sigma_3} = \frac{\sin \pi/n_3}{n_3} \sqrt{\frac{a_1 \csc \phi}{k}} \left\{ \left[\cos \frac{\pi}{n_3} - \cos \frac{2\phi}{n_3} \right]^{-1} \mp \left[\cos \frac{\pi}{n_3} - 1 \right]^{-1} \right\}$$
$$0 \leq \Phi \leq \Phi_3$$

$$= 0 \; ; \; \Phi > \Phi_3$$

$$\sqrt{\sigma_4} = \frac{\sin \pi/n_4}{n_4} \sqrt{\frac{a_2 \csc \phi}{k}} \left\{ \left[\cos \frac{\pi}{n_4} - \cos \frac{2\pi - 2\phi - 2 \times F_2}{n_4} \right]^{-1} \mp \left[\cos \frac{\pi}{n_4} - 1 \right]^{-1} \right\}$$

$$\sqrt{\sigma_5} = \frac{\sin \pi/n_2}{n_2} \sqrt{\frac{a_1 \csc \phi}{k}} \left\{ \left[\cos \pi/n_2 - \cos \frac{2\pi + 2\phi}{n_2} \right]^{-1} \mp \left[\cos \frac{\pi}{n_2} - 1 \right]^{-1} \right\}$$
$$0 \leq \Phi \leq \Phi_5$$

$$= 0 \; ; \; \Phi > \Phi_5$$

$$\sqrt{\sigma_7} = \frac{\sin \pi/n_4}{n_4} \sqrt{\frac{a_2 \csc\phi}{k}} \left\{ \left[\cos \pi/n_4 - \cos \frac{2\pi + 2\phi + 2x_{F_2}}{n_4} \right]^{-1} \mp \left[\cos \pi/n_4 - 1 \right]^{-1} \right\}$$

$$= 0 \; ; \quad \Phi_7 \leq \Phi \leq \Phi_8 \qquad \qquad 0 \leq \Phi \leq \Phi_7 \; ; \; \Phi_8 \leq \Phi \leq \pi$$

$$\mathcal{S}_2 = \pi/4 - 2k[a_1 \sin\phi + 2h_2 \cos\phi] \; ; \quad \mathcal{S}_3 = \frac{\pi}{4} - 2ka_1 \sin\phi$$

$$\mathcal{S}_4 = \frac{\pi}{4} - 2k[a_2 \sin\phi - 2h_3 \cos\phi] \; ; \quad \mathcal{S}_5 = -\frac{\pi}{4} + 2k[a_1 \sin\phi - 2h_2 \cos\phi]$$

$$\mathcal{S}_7 = -\pi/4 + 2k[a_2 \sin\phi + 2h_3 \cos\phi]$$

$$n_2 = 1 + \frac{x_c}{\pi} \; ; \quad x_c = \text{cone half angle}$$

$$n_3 = 1 - \frac{x_{F_1}}{\pi} \; ; \quad x_{F_1} = \text{flare segment halfangle}$$

$$n_4 = 1 + \frac{x_{F_1} + x_{F_2}}{\pi} \; ; \quad x_{F_2} = \text{Frustum halfangle}$$

$$k = 2\pi/\lambda$$

$$\Phi_2 = \pi - \tan^{-1} \frac{a_2 - a_1}{2(h_2 + h_3)} \qquad ; \quad \Phi_3 = \pi - \tan^{-1} \frac{a_2 - a_1}{2h_3}$$

$$\Phi_5 = \tan^{-1} \frac{a_1 - a_3}{2h_1} \; ; \quad \Phi_7 = \tan^{-1} \frac{a_2 - a_1}{2(h_2 + h_3)} \; ; \quad \Phi_8 = \pi - \tan^{-1} \frac{a_2 - a_F}{2h_4}$$

At a near nose on aspect angles scattering centers S_2 and S_5 (and S_4 and S_7) expand to form a ring discontinuity. The RCS may be given by:

$$\left[\sqrt{\sigma_2} e^{j\mathcal{S}_2} + \sqrt{\sigma_5} e^{j\mathcal{S}_5} \right] (\phi \approx 0) = \frac{\sin \pi/n_2}{n_2} 2a\sqrt{\pi} e^{-j4kh_2 \cos\phi} \left[\left\{ \cos \frac{\pi}{n_2} - \cos \frac{2\pi}{n_2} \right\}^{-1} \times \right.$$

$$J_0(2ka_1 \sin\phi) - j \frac{\frac{2}{\pi} \sin \frac{2\pi}{n_2} \tan\phi}{\left(\cos \pi/n_2 - \cos \frac{\pi}{n_2} \right)} J_1(2ka_1 \sin\phi) \pm \left\{ \cos \frac{\pi}{n_2} - 1 \right\}^{-1} J_2(2ka_1 \sin\phi) \Bigg]$$

$$\left[\sqrt{\sigma_4} e^{j\mathcal{S}_4} + \sqrt{\sigma_7} e^{j\mathcal{S}_7} \right] (\phi \approx 0) = 2\sqrt{\pi} a \frac{\sin \pi/n_4}{n_4} e^{j4kh_3 \cos\phi} \times$$

$$\left[\left\{ \cos \pi/n_4 - \cos \frac{2\pi - 2x_{F_2}}{n_4} \right\}^{-1} \times J_0(2ka_2 \sin\phi) - j \frac{\frac{2}{n_4} \sin \frac{2\pi + 2x_{F_3}}{n_4} \tan\phi}{\left(\cos \pi/n_4 - \cos \frac{2\pi + 2x_{F_2}}{n_4} \right)} \times \right.$$

$$J_1(2ka_2 \sin\phi) \pm \left\{ \cos \pi/n_4 - 1 \right\}^{-1} J_2(2ka_2 \sin\phi) \Bigg]$$

At the tail-on and near tail-on axail aspect, scattering centers S_4 and S_7 again expand to form a ring discontinuity. Then one may have:

$$\left[\sqrt{\sigma_4}\, e^{j S_4} + \sqrt{\sigma_7}\, e^{j S_7}\right](\phi \approx \pi) = 2\sqrt{\pi}\, a\, \frac{\sin \pi/n_4}{n_4}\, e^{-j k_4 h_3 \cos\phi} \times$$

$$\left[\left\{\cos \pi/n_4 - \cos 2xF_2/n_4\right\}^{-1} \times J_0\left(2 k a_2 \sin\phi\right) - j\, \frac{\frac{2}{n_4}\sin\frac{2xF_2}{n_4}\tan\phi}{\left(\cos \pi/n_4 - \cos \frac{2xF_2}{n_4}\right)^2} \times \right.$$

$$\left. J_1\left(2 k a_2 \sin\phi\right) \pm \left\{\cos \pi/n_4 - 1\right\}^{-1} J_2\left(2 k a_2 \sin\phi\right)\right]$$

For the broadside case ($\phi = \pi/2$), the RCS expression may be written as

$$\left[\sqrt{\sigma_2}\, e^{j S_2} + \sqrt{\sigma_4}\, e^{j S_3}\right](\phi = \pi/2) = \left[- \sqrt{k a_1}\, 2 h_2 \frac{\sin(2 k h_2 \cos\phi)}{(2 k h_2 \cos\phi)}\, e^{j 3n_4 - j2 k h_2 \cos\phi}\right.$$

$$\mp \sqrt{\frac{a_1}{k}}\, e^{j \pi/4}\left\{\frac{1/n_2 \sin \pi/n_2}{\cos \pi/n_2 - 1}\, e^{-j 4 k h_2 \cos\phi} + \frac{\frac{1}{n_3}\sin \pi/n_3}{\cos \pi/n_3 - 1}\right\}\right] \times$$

$$e^{-j2 k a_1 \sin\phi}$$

ANALYTICAL PLOTS

The RCS expressions were run on a digital computer with a target dimensions (in inches) for test calculations shown as below:

$$a_1 = .90'', \qquad a_2 = 1.70''$$
$$\text{and} \quad \lambda = 1.70''$$

These results are plotted in figures 3. and 4.

INTERPRETATION OF RESULTS

The observed dincontinuties in the predicted RCS indicate aspects for which further modification of geometrical diffraction theory is required. The discontinuity observed for $\emptyset = 5.6$ degrees is due to the shadowing of ring discontinuity by the contribution due the scattering center S_4 and S_7 of Figure 2. For $\emptyset = 75.6$ degrees, one may replace the return from this ring discontinuity by the contribution due to scattering center S_4, according to equations 14 and 24. The discontinuity observed for $\emptyset = 10$ degrees is due to the shadowing of scattering center S_5. Multiple diffraction consideration will allow smooth transition here. Two singularities remain in the formulation sue to the use of unmodified geometrical diffraction theory in describing specular scattering by conical surfaces. The effects of these singularities are the two spikes occuring at $\emptyset = 74.5$ degrees (due to the cone specular) and at $\emptyset = 70$ degrees (the specular from the flare). Since the theory fails gracefully for conical speculars, physical optics estimates may be introduced in a small angular region centered about specular aspect. The remaining discontinuity occurs at $\emptyset = 117$ degrees, at which aspect, the return from the ring singularity

is introduced. In actual fact, this ring contribution is valid for aspect with 15 degrees of the tail-on axail aspect since it is based upon small angle approximation.
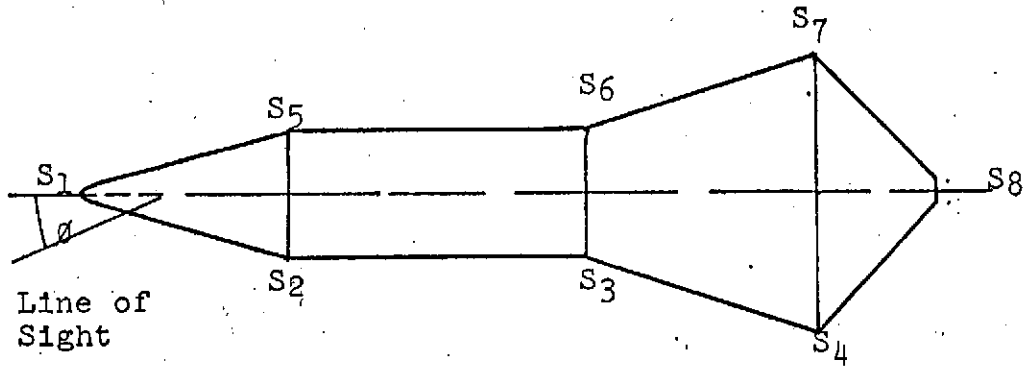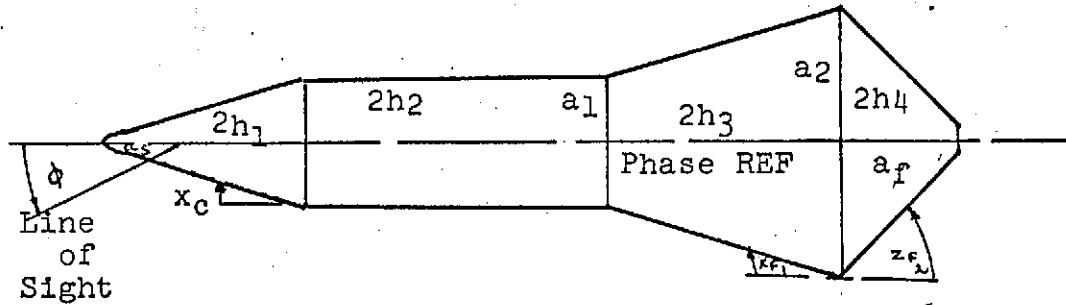
Fig. 1. Scattering Centers On Composite Body
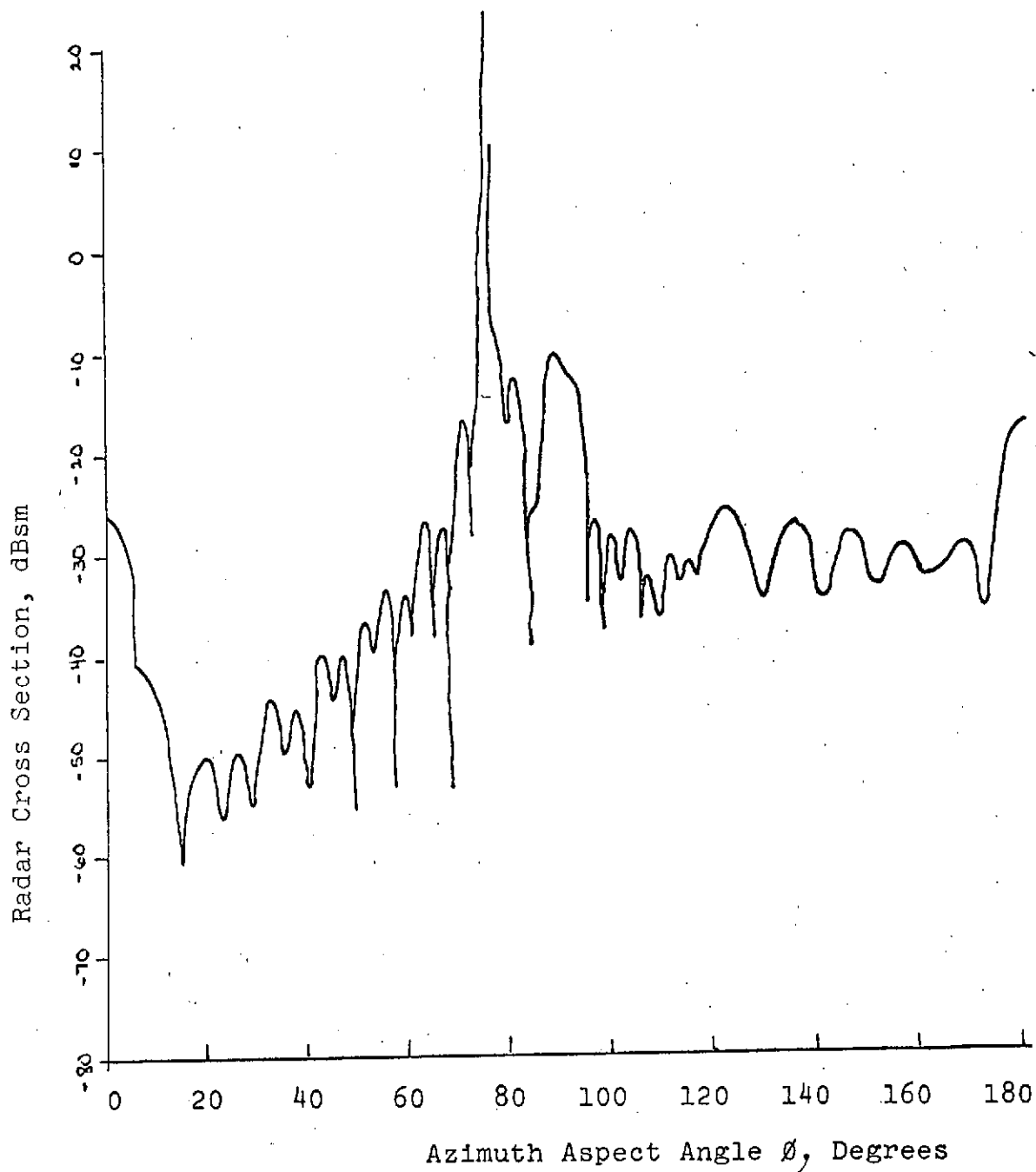

Fig. 2. Composite Geometry

Fig. 35 Radar Cross Section of Composite body, Vertical Polarization.
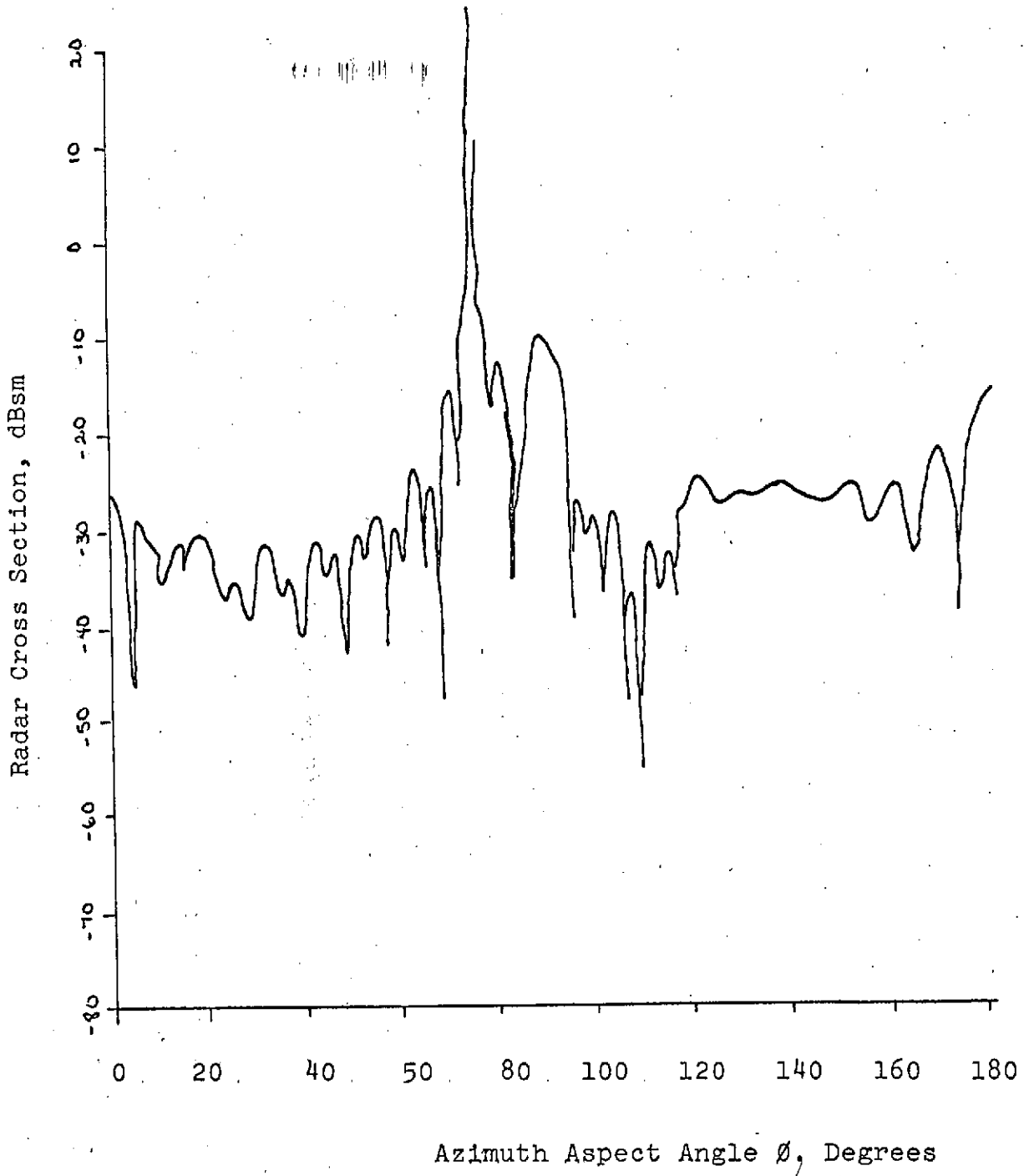
Azimuth Aspect Angle Ø, Degrees

Figure 4. Radar Cross Section Of Composite Body, Horizontal
Polarization

RADAR CROSS SECTION ESTIMATION FOR COMPLEX SHAPES

This study presents a method for estimating RCS of complex shapes such as an aircraft, missle, and satellite. It is based upon methods already developed for simple shapes. The theoretical method for estimating the RCS of complex shapes utilizes the following steps.

1. The complex shape is resolved into an ensamble of components each of which can be geometrically approximated by a simple shape in such a way that the RCS of simple shape approximates the RCS of the component it replaces.

2. RCS values are computed for the approximations to the components (simple shapes) derived in step (1).

3. Steps (1) and (2) are then combined to yield an estimate of the RCS of entire body.

Two methods i. e. "relative phase method" and "random phase method" are proposed. Furthermore, theoretical results are compared against the experimental results.

TARGET AND COORDINATE SYSTEM

Two targets are investigated:

A missle model is shown in Fig. 1.

An aircraft model is shown in Fig. 2.

ANALYTICAL EXPRESSIONS

Relative Phase Method - For any given combination of aspect angle, wave length, and polarization, N components for which

RCS values have been computed, e. g., the set of values.

$$\sigma_1, \sigma_2, \sigma_3, \bullet \quad \bullet \quad \bullet, \sigma_N$$

One of the methods of combination involves the consideration
of the relative plase angle between the returns from these N
scatters. Therefore, the RCS of the entire body may be written
as:

$$\sigma_p = \left| \sum_{j=1}^{N} (\sigma_j)^{1/2} \exp(j\phi_j) \right|^2$$

where σ_j = the RCS of the jth component and ϕ_j = the re-
lative phase angle associated in the jth component.

RANDOM PHASE METHOD– In case where ϕ_j are randomly distributed,
then upon averaging over the ϕ_j , one obtains the expressions:

$$E[\sigma] = \sum_{j=1}^{N} \sigma_j$$

$$E[\sigma] \pm S$$

$$S^2 = \left(\sum_{j=1}^{N} \sigma_j \right)^2 - \sum_{j=1}^{N} \sigma_j^2$$

ANALYTICAL AND/OR EXPERIMENTAL PLOTS

For the case of a Missle, results are shown in Figs. 2,

-3, and -4, and for the case of a large jet-aircraft, results are shown in Figures 6 and 7.

INTERPRETATION OF RESULTS

It may be noted that relative phase method is not good for large aircrafts at small wavelengths. In such cases random phase method should be used. Techniques discussed here are most effective tools with which to describe modification, and even the design of RCS characteristics of complex shapes.
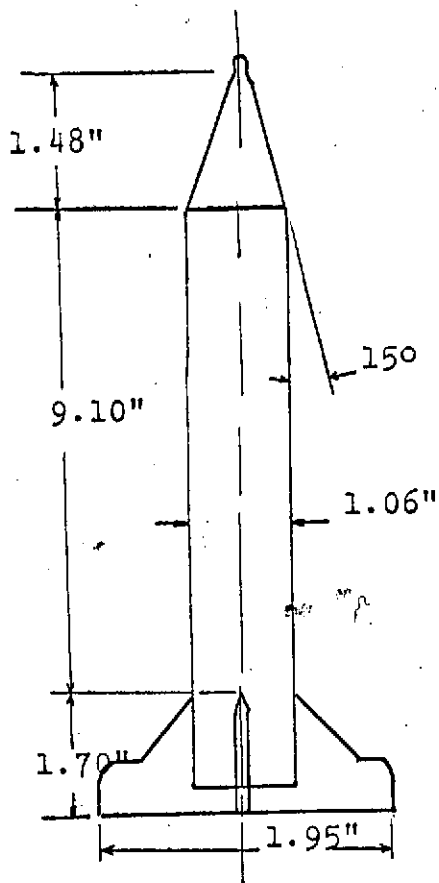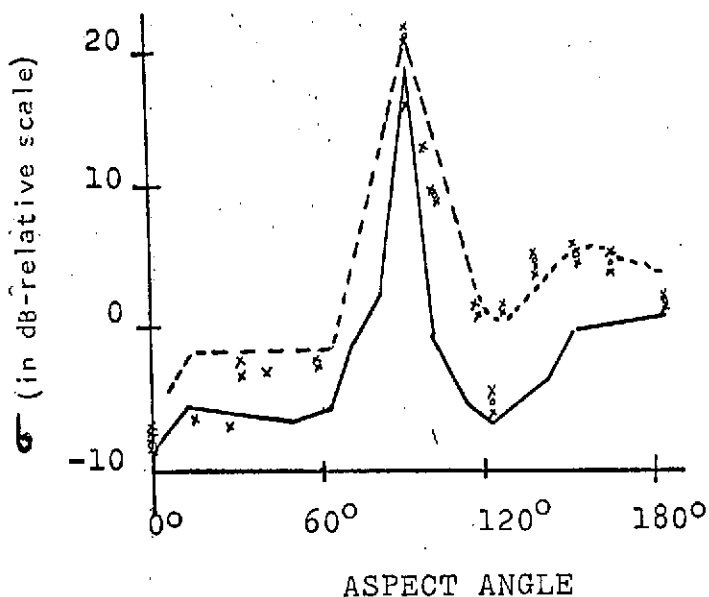
Fig. 1.   Sketch of missile model.

ASPECT ANGLE

Fig. 2.   Missile with fins——theory and experiment for
vertical polarization (E vector normal to plane in
which aspect is measured, two of the fins contained in
that plane). X X X experimental points;- - -theory (in
phase estimation);————theory (random phase estimation).
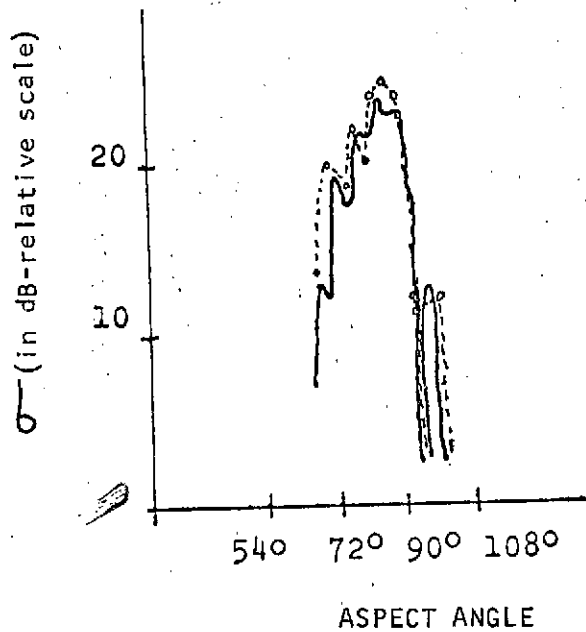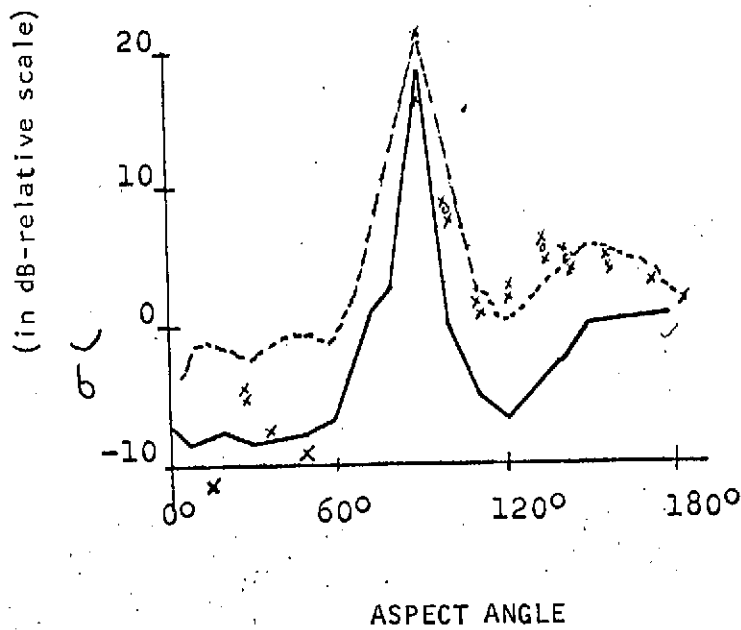
ASPECT ANGLE

ASPECT ANGLE

Fig. 3. Missile with fins_, theory and experiment for
E vector slanted at a 45° angle to the plane in which
aspect is measured (two fins located in that plane).
X X X Experimental points;----theory (in-phase esti-
mation);_____theory (random phase estimation).

Fig. 4. RCS for a missile near broadside._____ Ex-
perimental data; . . . theory (relative phase).
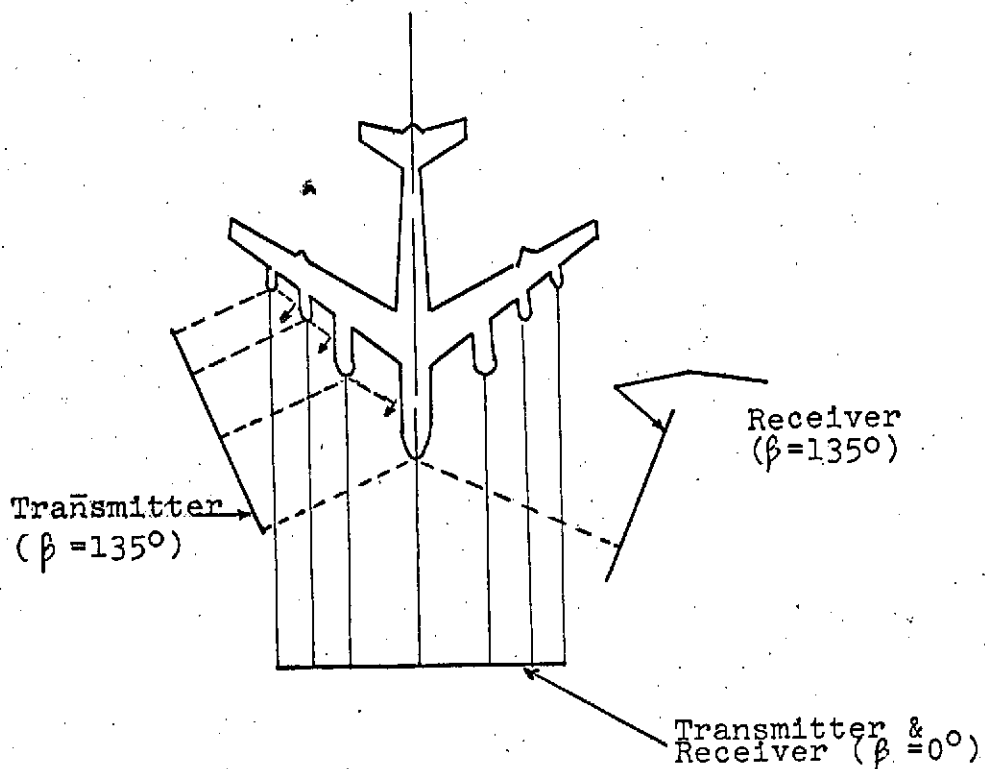
Fig. 52. Monostatic and bistatic scattering from the nose
of a large aircraft (the $\theta=0°$ case for $\beta=0°$ and $\beta=135°$).

(in dB-relative scale)

10° Median Values

Maxima

(a) θ →

(a) θ →

10° Maximum Values

Minima

(b) θ →

(b) θ →
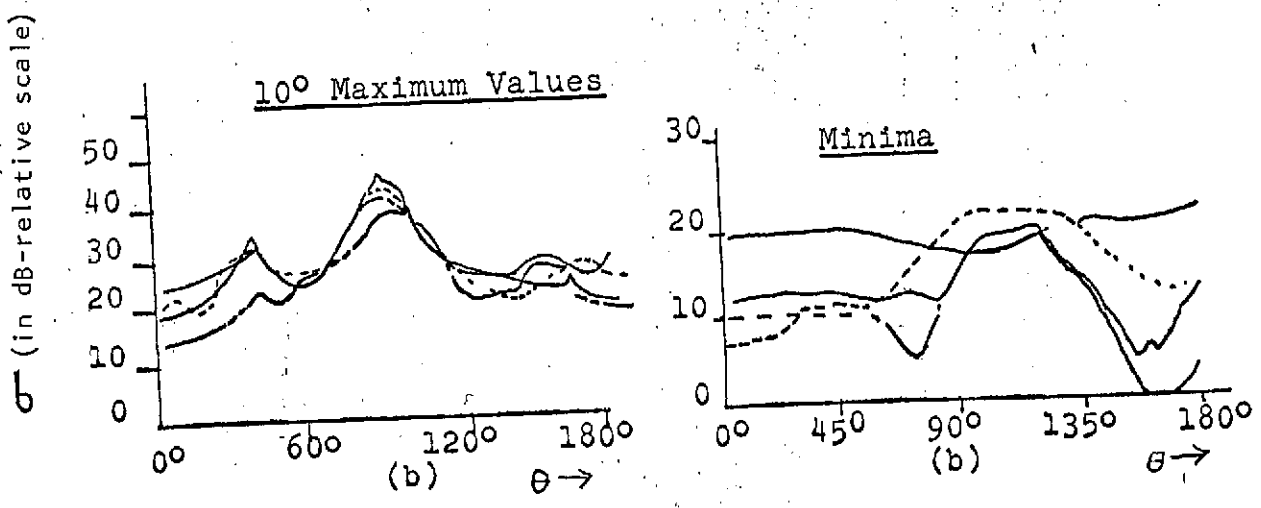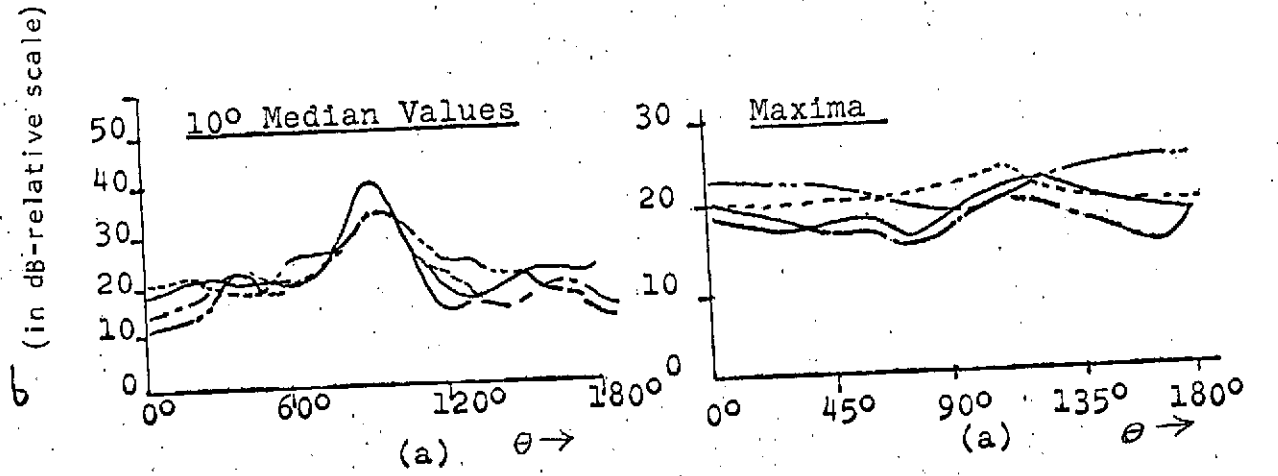
Fig. 6. Bistatic RCS of a
large jet aircraft at 250
MHz (horizontal polariza-
tion). ——— β=0°; ——— β=30°;
——·—— β=60°; ——··—— β=135°

Fig. 7. Bistatic RCS o
a missile shape at 200
MHz (horizontal polari
zation). ——— β=0°; ——·—
β=40°; ——— =90°;
β——··—·· =150°.

COMPUTERIZED RAY OPTICS METHOD OF CALCULATING AVERAGE VALUE RADAR-CROSS-SECTION

In order to estimate the RCS of airborne vehicles, it is often necessary to consider the average values of radar returns. A method providing the quick estimate of the average static radar cross section of the vehicle components would ve useful. This study extends a method of ray optics called computerized ray optics method to determine the RCS of a body of arbitrary shape, and which may be concave and/or convex on which double reflection and depolarization can occur. The reason for this method can be used here on an arbitrary body is that rather than finding an expression for the RCS, a large number of rays are simply "thrown" at the body. The reflection boundary conditions for a perfect conductor (Etangential = 0, and Dnormal are continuous) collected at the receiver and summed (vector-wise and phase-wise). Analytical results are compared against the experimented results.

TARGET GEOMETRY AND/OR CONDUCTIVE SYSTEM

The explanation of the target and coordinate system used is shown in Figs. 1, 2, and 3.

ANALYTICAL EXPRESSIONS

The bistatic radar cross section is defined as:

$$\sigma_\theta \ (\theta_{nom}, \phi_{nom}) = \left(P_\theta \ (\theta_{nom}, \phi_{nom}) \middle/ d\Omega \right) \middle/ (P_{in}/4\pi)$$

$$\sigma_\theta = \frac{4\pi \sqrt{\left[\sum_{ALL\ RAYS} Re(P_\theta)\right]^2 + \left[\sum_{ALL\ RAYS} Im(P_\theta)\right]^2}}{(d\Omega)(N)(P_2')}$$

$$\sigma_\phi = \frac{4\pi \sqrt{\left[\sum_{ALL\ RAYS} Re(P_\phi)\right]^2 + \left[\sum_{ALL\ RAYS} Im(P_\phi)\right]^2}}{(d\Omega)(N)(P_2')}$$

where
$$P\theta = Re\ (P\theta) + j\ Im\ (P\theta)$$
$$P\emptyset = Re\ (P\emptyset) + j\ Im\ (P\emptyset)$$

P_2' is the power in the 2nd incident ray and is equal to unity and N
is the number of rays per square meter.

EXPERIMENTAL DETAILS

An experimental body is shown in Fig. 3. It is composed of an
ogive "O", a cylinder "C", a hemisphere "S", and a winglike body "W".
It was is to test the method of computerized ray optics to calculate
average values of RCS of bodies that can display 1) interference
phenomena, 2) double reflections, and 3) depolarization.

ANALYTICAL AND/OR EXPERIMENTAL PLOTS

The analytical and experimental plots are shown in Fig. 4.

INTERPRETATION OF RESULTS

The analysis shows that agreement between measured and calculated
results in generally good and within $\pm$ 2dB, except at $\theta = 0$, $\emptyset = 0$,
where a crepting wave was identified experimentally. The angles at

which large creeping wave will be excited can be predicted

by observing the angles of glancing incidence at a discontinuity

of the surface.
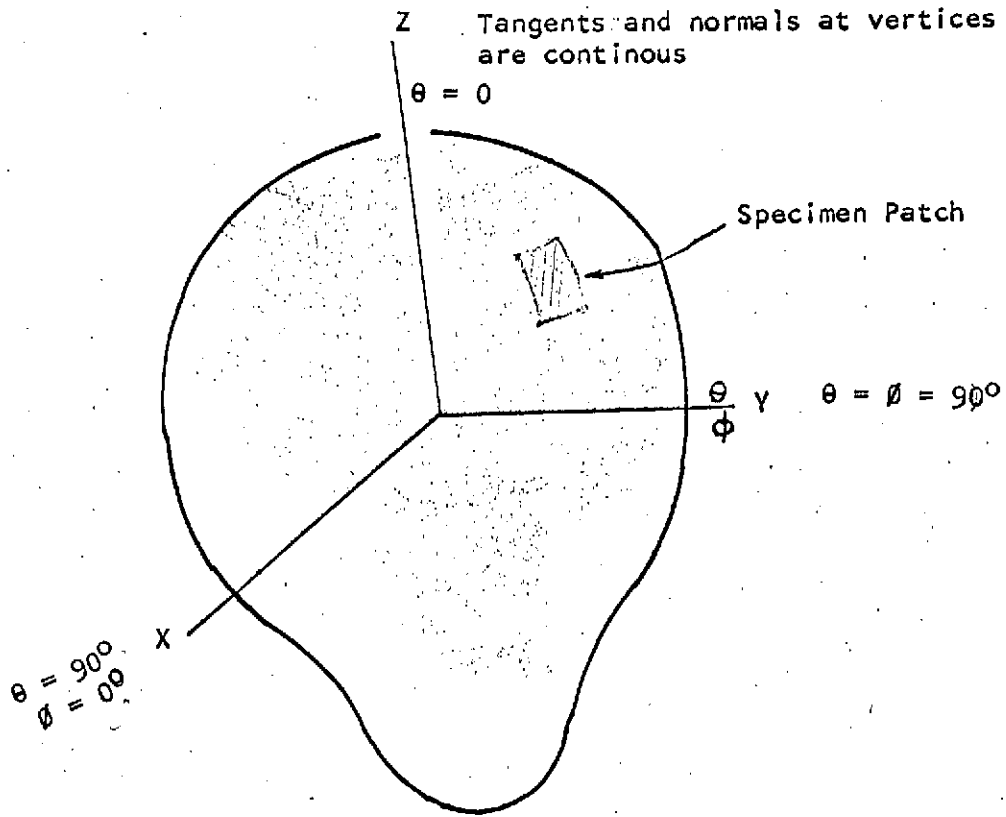
Fig. 1. Arbitrary body defined by patchwork surface.
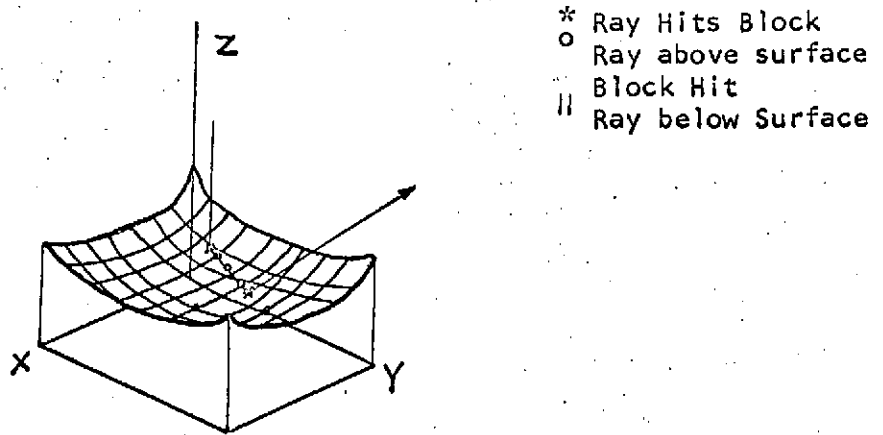
Fig. 2. Double reflection.

X

θ = 90°
∅ = 0°

θ = 180

Y   θ = 90°
     ∅ = 90°

Z

θ = 0°

Fig. 3.   Experimental body.

Radar cross section
(dB relative to 1.0 m²)

+20

• ——— • Computed average
        10° median
——— freq 10 Ghz

0

-20

-30

180   60   60   180
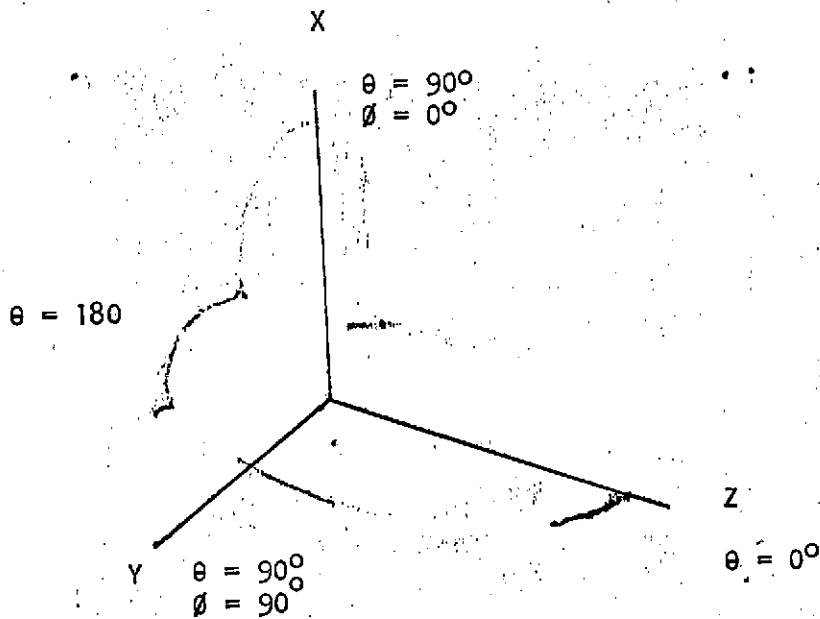
Fig. 4.   Monostatic radar cross section versus θ for ∅ =0
          and ∅ = 180° at 10.0 GHz for body 1.

COMPARASION OF RCS BY MICROWAVE AND OPTICAL SIMULATION TECHNIQUES

Radar cross section of a jet aircraft is obtained using microwave and optical simulation techniques.

TARGET AND COORDINATE SYSTEM

$(\frac{1}{4})$ scale model of a modern jet aircraft is used.

EXPERIMENTAL DETAILS

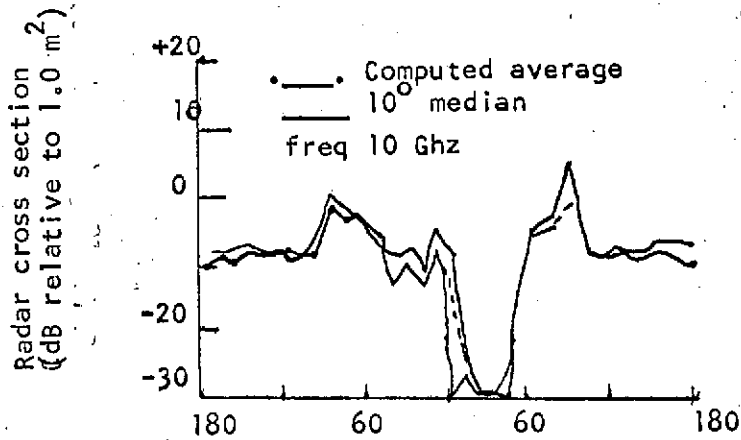Mictowave measurement are undertaken using a (cw) balanced-bridge RCS measurement system at 4.4 GHz, and $(\frac{1}{4})$ scale model of a modern jet aircraft model to simulate quasi-monostatic RCS measurements at 8.6 GHz of the full scale aircraft.

The optical simulation measurements are conducted using a monostatic optical simulation system and $(1/35)$ scale model of the same aircraft. The model was loaded with vacum deposit aluminium producing a mirror like surface.

EXPERIMENTAL PLOTS

The results obtained from both these techniques are plotted in Fig. 1.

INTERPRETATION OF RESULTS

The mean radar-cross-sections are considered to be valid for frequencies between 3GHz and 24 GHz. Results of measurement agree with in an average of 3.5 dB and that both techniques can be used to obtain RCS at microwave frequencies of complex shapes such as aircraft.
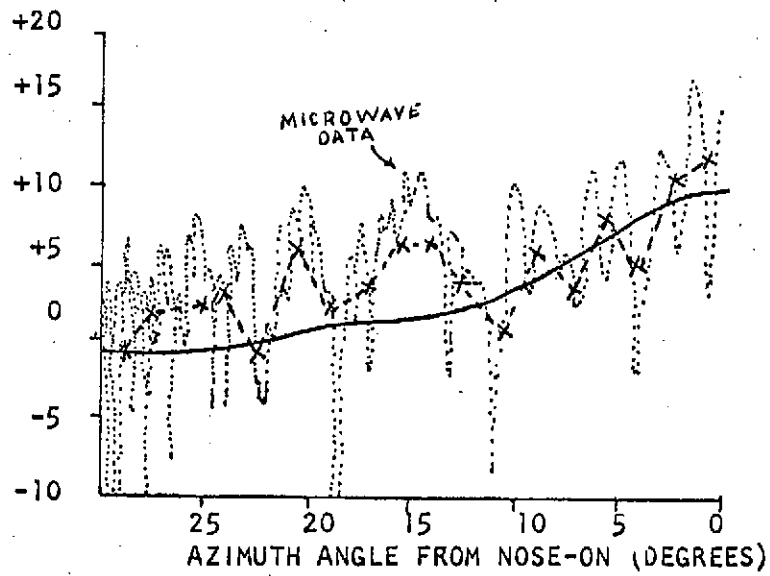
Fig. 1. Comparison of radar cross-section data from optical simulation and microwave measurements.

B I B L I O G R A P H Y

M. E. Becthel, "Application of Geometrical Diffraction Theory
to Scattering From Cones and Disks", Proceedings of the
IEEE, August, 1965.

M. E. Becthel and R. A. Ross, "Handbook of Scattering Coefficients",
CAL Report No. UF2457-E-1, Cornell Aeronautical Laboratory,
Inc., Buffalo, N. Y., November, 1967.

M. E. Bechtel and R. A. Ross, "Radar Scattering Analysis", CAL
Report No. ER/RIS-10, Cornell Aeronautical Laboratory, Inc.,
Buffalo, N. Y., August, 1966.

R. W. Chynoweth, and R-RBooth, "An Analytical Determination of
the Radar-Cross-Section of Certain Missle like Configurations",
U. S. Army Missle Command, Redstone Arsenal Rept. No.
RF-TR-63-16, 13 August 1973.

J. W. Crlispin Jr., and A. L. Maffett, "The Practical Problem of
Radar Cross Section Analysis", IEEE Trans. on Aerospace and
Electronics Systems, pp. 392-395, March 1971.

J. W. Crispin Jr. and K. M. Siegel, Methods of Radar-Cross-Section
Analysis, Academic Press, New York, 1968.

J. W. Crispin Jr. and A. L. Maffett, "Radar Cross Section Estimation for Complex Shapes, Proceedings of the IEEE, August, 1965.

J. B. Keller, "Geometrical Theory of Diffraction", J. Opt. Soc. Amer., vol. 52, pp. 116-130, February 1962.

R. E. Kell, "On the Derivation of Bistatic RCS from Monostatie Measurements", Proc, IEEE, vol. 53, pp. 983-988, August 1965.

E. F. Knott and T. B. A. Senior, "Cross Polarization Diagnostics", IEEE Trans. on Antennas and Progation, March 1972.

J. K. Kojendal, "Comparision of RCS by Microwave and Optical Stimulation Techniques", August 1965.

R. G. Kouyoumjian, D. T. Thomas, and L. Peters Jr., "A Modified Geometrics Optics Method for Scattering By Dielectric Bodies", IEEE Trans. on Antennas and Propogation, vol. AP-11, pp. 690-703, November, 1963.

T. Matsuyuki and Y. Suzuki, "Measurement of Radar Cross Section by Phase Interfrence Method", Defense Academy, Yokosuka, pp. 60-69, February 26, 1966.

C. R. Mullon, R. Sandburg, and C. O. Velline, "A Numerical Technique for the Determination of Scattering Cross Sections of Arbitrary Geometrical Cross Section", IEEE Trans. on Antennas and Progation, January, 1965.

F. W. Oshiro, K. M. Nitzner, and et'al, <u>Calculation of Radar-Cross-Section-Part 11.Analytical Report</u>, AFAL-TR-70-21, Part 11, Wright-Patterson Air Force Base, Ohio, April, 1970.

L. Peters, Jr., and F. C. Weiner, "Concerning the Assumption of Random Distribution of Scatterers as a Model of an Aircraft", IRE Trans. on Antennas and Propagation, vol. AP-9, pp. 110-111, January 1961.

L. W. Peters, T. Kawanao, and W. G. Swarner, "Approximation for Dielectric or Plasma Scatterers, August, 1965.

D. M. Raybin, "Radar Cross Section of Spherical Shell Segments", IEEE Trans. on Antennas and Progation, September, 1965.

<u>Reference Data For Radio Engineers</u>, Forth Edition, International Telephone and Telegraph Corporation, New York, 1950.

B. J. Roscoe and J. F. Banas, "Cross Section of Blunted Cones", Proc. IEEE, V61, n11, November, 1973.

R. A. Ross, C. C. Freeny, and J. C. Cleary, "Bistatic Scattering Matrix for a Finite Right Cicurlar Cylinder", Electronics Letters, vol. 4, April 1968.

R. A. Ross, "Bistatic Scattering Matrix for a Frustrum", IEEE Trans. on Antennas and Progation, January, 1969.

R. A. Ross, "Radar Cross Section of a Finite Rectangular Cylinder", Electronics, Letters, July, 1967.

R. A. Ross, "Radar Cross Section of Rectangular Flat Plates as a
Function of Aspect Angle", IEEE Trans. on Antennas and Proga-
tion.

R. A. Ross, "Scattering By a Finite Cylinder", Proc., IEEE, vol. 114,
pp. 864-868, 1967.

R. Alexander Ross and Howard R. Witt, "Investigation of Scatter-
ing Center Theory", CAL Report No. UA-2464eE-1, Wright-
Patterson Air Force Base, Ohio, July, 1967.

R. A. Ross and M. E. Bechtel, "Scattering-Center Theory and Radar
G
Glint Analysis, IEEE Trans. on Aerospaceeand Electronids Systems,
vol. AES-4, No. 5, pp. 756-762, September, 1968.

T. Ruck, D. E. Barrick, et al, Radar-Cross-Section Handbook-Volumne I
and II, Plenum Press, New York, 1970.

T. B. A. Senior, "Diffraction Coefficients for a Discontinuity
in Curvature", Electron Lett., vol. 7, pp. 249-250, May 20, 1971.

T. B. A. Senior P. L. E. Uslanghi, "High- Frequency Backscattering
from a Mehalic Disk", Proc. Inst., Elec. Eng., December, 1971.

T. B. A. Senior, "Low Frequency Scattering by a Finite Cone",
Journal of Applied Science Research, vol. 23, March 1971.

T. B. A. Senior, "The Backscattering Cross Section of a Cone Sphere",
IEEE Trans. on Antennas and Propagation, pp. 271-277, March 1965.

C. F. Stubenrauch and C. T. Tai, "Dyadic Green's Functions for
Cylindrical Waveguides with Moving Media", Journal of Applied
Science Research, vol. 25, pp. 281-289, December 1971.

J. F. Sulan, "C-Band Radar Cross Section for Spacecraft", TRW Tech
Rept. No. 05952-H463-PO-00, Houston, Texas, April 1, 1968.

W. G. Swarner, and L. Peters, Jr., "Radar Cross Sections of
Dielectric or Plasma Coated Conducting Bodies", IEEE
Trans. on Antennas and Propagation, vol. AP-11, pp. 558-569,
September, 1963.

P. L. E. Uslenghi, "The Backscattering RCS of Long, Thin Dielictric
Bodies of Revolution on a Metal Plane", Canadian Journal of
Physics, June, 1965.

S. F. Weiner and S. L. Borison, "Radar Scattering from Blunt Cone
Tips", IEEE Trans. on Antennas and Progation, November, 1966.

M. R. Weiss, "Numerical Evaluation of Geometrical Optics Radar
Cross Section", IEEE Trans. on Antennas and Propagation,
pp, 239-241, March 1969.

D. W. White, "Radar Simulation and Analysis By Digital Computer",
John Hopkins University, Applied Physics Lab, Baltimore,
M. D., TG-952, 1968.